HOW DOES A FEAR ENGRAM INFLUENCE BRAIN AND BEHAVIOR STATES

Antje R. de Boer

Supervised by Steve Ramirez, Robbert Havekes and Kaitlyn Dorst

Abstract

Negative affective states are believed to contribute to psychiatric disorders. Studying the neural circuitry of fear behavior can provide insights into the underlying mechanisms of these disorders. The aim of this study was to explore the neuronal networks that are involved in fear memory and defensive behaviors by investigating how a fear engram influences both brain and behavior states. We did this by observing and manipulating the activity of relevant brain areas during the reactivation of fear memory-bearing engram cells. We optogenetically reactivated a tagged fear engram in the dentate gyrus (DG) subregion of the hippocampus and tested the effects of chemogenetic inhibition of the lateral hypothalamus (LHA) on light-induced freezing and cFos expression. Additionally, we examined light-induced freezing behavior and neuronal activity of the periaqueductal grey (PAG) during optogenetic reactivation of a tagged fear engram in differently sized environments. Based on the results, we conclude that LHA activity is necessary for freezing behavior as inhibiting the LHA eliminated freezing behavior. We also conclude that animals freeze more in a small environment than in a large environment. Lastly, we conclude that the reception of a foot shock increases PAG neuronal activity. By unraveling the contributions of the LHA, PAG, and environmental factors in fear behavior, this research provides valuable insights into the neural circuitry underlying fear. These findings have significant implications for the development of treatment strategies that target disorders characterized by abnormal fear and anxiety responses.

Contents

1. Introduction

1.1 The Costs of Psychiatric Disorders on Quality of life and Society

Psychiatric disorders impact mood, behavior, and cognition and decrease the quality of life of the patients that suffer from them. These disorders are globally ranked fifth in leading causes of disability, largely through their significant impact on disability-adjusted life years (DALYs) (Figure 1). This is a measure of the years lost due to poor health, disability, or premature mortality (Sullivan & Geschwind, 2019; Saarni et al., 2007). Psychiatric disorders can have large negative financial, physical, and emotional consequences for the individual and society at large (Kessler et al., 1995; Schmidt et al., 2008).

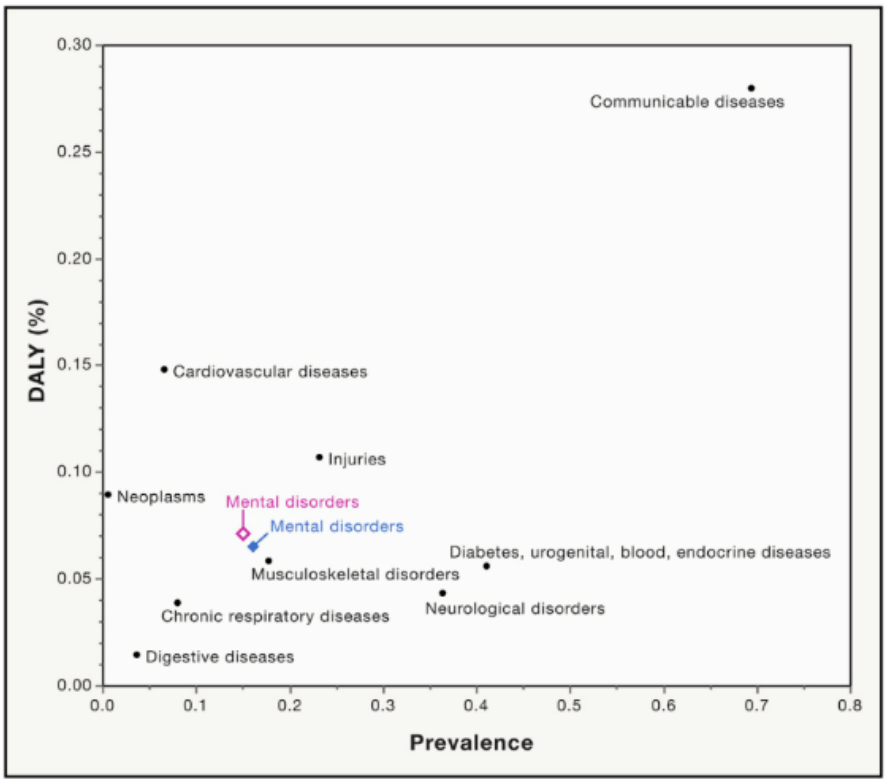

Figure 1. Prevalence and Impact of psychiatric disorders compared to other major disorders (Taken from Sullivan & Geschwind, 2019)

An example of a group of psychiatric disorders that greatly influences life quality is anxiety disorders (ADs). ADs affect approximately 275 million people, making them one of the leading causes of disease burden worldwide (Vos et al., 2017). Because ADs are characterized by anxiety and fear, they negatively affect the lives of the patients. This is also shown by a meta-analysis as they found that quality of life is significantly lower among patients with an anxiety disorder than among nonclinical controls (Olatunji et al., 2007). Patients are faced with financial problems, impairment in education and relationships, and high rates of divorce and disability which show that ADs negatively impact functional areas that contribute to quality of life (Weissman, 1991; Stein & Kean, 2000; Robbins et al., 1991). These disorders also affect society at large by increasing healthcare costs as a meta-analysis shows that, on an individual level, healthcare costs in patients with acute ADs are twice as high as in individuals without ADs (Konnopka & König, 2020). Many other psychiatric disorders show the same effects on quality of life and society. For example, individuals with major depression also have been found to have a lower subjective quality of life (Hansson, 2002).

These psychiatric disorders greatly influence the lives of the patients, but also negatively impact society. Because of this, a lot of research has been dedicated to unraveling the causes and underlying neuronal circuitry and processes that could mitigate or prevent these pathological phenotypes.

In this thesis, first some background information will be provided on negative affective states, fear and defensive behavior, and the influence of environment on fear behavior. Then, different brain areas that are involved in fear behavior will be described, including the hippocampus, lateral hypothalamus, and periaqueductal gray, alongside recent research on engram cells. Afterwards, the research questions and hypotheses will be presented, followed up by the research methods, results and discussion. By investigating these topics, this thesis aims to provide insight into the causes and potential prevention or mitigation of psychiatric disorders.

1.2 The Role of Negative Affective States in Psychopathology

Psychiatric disorders are a major challenge for both individuals and society at large and patients that suffer from these disorders experience negative affective states. By investigating these negative affective states, more can be learned about psychiatric disorders.

Negative affect (NA) is a broad term that is used to describe a range of negative emotions and feelings of distress. Negative affective states, such as behavioral despair, anhedonia, heightened stress reactivity, decreased motivation, and dysphoria, are observed in many neuropsychiatric disorders such as depression, bipolar disorder, anxiety and mood disorders, and post-traumatic stress disorder (Tejeda & Bonci, 2019). At a trait level, a predisposition to experiencing negative emotions is referred to as negative affect (NA) (Watson & Clark, 1984). Problems with controlling intense, negative, and changing emotional states may play a role in various types of mental disorders. This is shown by the fact that patients with psychiatric disorders generally display higher NA scores than healthy controls (Table 1) and are more likely to be distressed and upset and have a negative view of self (Watson & Clark, 1984). Furthermore, abnormalities in the neural systems that are important for the processing of negative effects have been associated with specific symptoms of schizophrenia and bipolar and major depressive disorder (Phillips et al., 2003).

Table 1. **Comparisons of Mean Negative Affectivity Levels among Diagnostic groups and healthy controls showing that neuropsychiatric patients have a higher negative affect score than controls** (Taken from Watson & Clark, 1984)

Subject	No. comparisons where: A > B	A = B	B > A
Patients vs. controls			
Inpatients	2	1	0
Mixed neurotic	9	0	0
Neuropsychiatric/ mixed	5	0	0
Depressives	4	0	0
Mental health clinic	3	0	0
Outpatients	2	0	0
Schizophrenic	1	2	0
Manic	0	1	1
Character disorders	2	1	0
Drug/alcohol abusers	3	1	0
Prisoners	3	2	0
Various medical groups	10	2	0
College student/adult counselees	6	0	0
Total	50	10	1

It seems that persistent negative affective states could be contributing to these psychiatric disorders. Because of this, a lot of research has been performed to find the neurological underpinnings and behavioral manifestations of emotion dysregulation.

1.3 The Biology of Fear: How do Individuals Respond to Threatening Stimuli

Fear behaviors have been used to investigate the behavioral manifestations of negative affective states because anxiety and stress are related to fear (Patriquin & Mathew, 2017; Maeng & Milad, 2017). However, fear behavior is very complex, and many different behavioral responses can be employed as a response to a fearful stimulus. To understand how we can use fear behavior to investigate the neurological mechanisms underlying psychiatric disorders, it is important to understand where fear behavior comes from, in what ways it can express itself and what factors influence it.

Defensive responses are the most common and frequently utilized behavior patterns for most animal species (Blanchard & Blanchard, 2008). Protective mechanisms are essential in extreme, life-threatening situations, but also in everyday life (Graziano & Cooke, 2006). In mammals, defensive responses can range from a somewhat straightforward startle reflex to sophisticated reactions that depend on the location of the harmful stimulus and the configuration of the limbs (Koch, 1999; Clarke

& Harris, 2004). Humans also show a variety of responses when exposed to a threat. This includes attentive freezing, a startle reflex, bradycardia, and active avoidance behavior (Löw et al., 2015). Freezing is defined as the absence of movement except for respiration (Curzon et al., 2011). Laboratory rodents show at least five defensive behaviors: flight, freezing, defensive threat, defensive attack, and risk assessment (Blanchard et al., 2001). Interestingly, looking at context, features of the threat of the stimulus, and the type of defensive behavior that an individual choses, the patterning of defensive behavior for humans and non-human mammals are very similar (Blanchard et al., 2001).

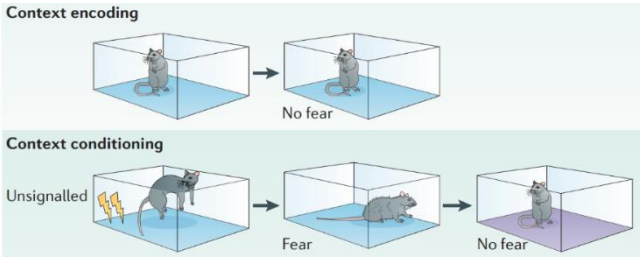

Figure 2. Context conditioning in rodents (Adapted from Maren et al., 2013)

Fear in laboratory animals can be studied by using a context fear conditioning (CFC) paradigm (Konorski, 1948). This paradigm pairs an initially neutral context with a stimulus that is intrinsically aversive. For example, an animal can be placed in a neutral context where it experiences a foot shock. The animal will then associate this context to the experience and the neutral context becomes the conditioned context and subsequently will elicit a fear reaction (Figure 2) (Beckers et al., 2013).

Through the research of laboratory animals such as rodents, the defense response of these animals can be further uncovered. To be able to use CFC and defensive responses to investigate the neuronal underpinnings of psychiatric disorders, it is useful to know how and when animals employ which defensive behaviors. According to the defense-cascade model, there are three stages of defensive behavior. Depending on the degree of the threat and the distance between the predator and prey, specific responses proceed in sequence along a scale (Figure 3) (Fanselow & Lester, 2013). The three stages are pre-encounter, post-encounter, and circa-strike. The pre-encounter phase occurs when an animal moves from safety to a context where a threat could be encountered. During this phase, the animal will show and preemptive behavior, including threat-nonspecific vigilance (Lang et al., 1997). Then, if a threat is detected, the animal will go into the post-encounter mode. Here, attention will be directed to the threat and more specific defensive responses will be employed such as fear bradycardia, potentiation of the startle reflex, and motor freezing (Fanselow, 1994). When the threat is most imminent, for example when a predator is approaching, passive defensive behavior (freezing) is switched out for active defensive behavior (fight or flight) (Fanselow, 1994). During fear conditioning, rodents show the different stages of the defense cascade model. The pre-encounter phase occurs when the animals are placed in the neutral context. After this, the animal will pair the neural context with an aversive stimulus transforming the neutral context into the conditioned context. The post-encounter phase occurs when an animal is placed in this conditioned context. Lastly, when the animal is experiencing the aversive stimulus, for example a foot shock, the circa-strike phase takes place. Behaviors within each mode increase until the next set of behaviors emerge (Fanselow, 1989; Helmstetter & Fanselow, 1993).

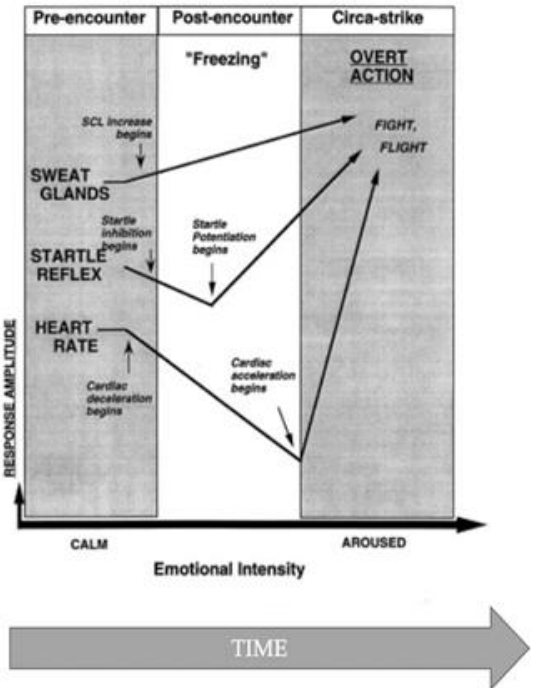

Figure 3. Threat-imminence and defense-cascade mode (Adapted from Lang et al.,

Overall, fear behavior mostly is a robust fundamental survival mechanism that can be studied and elicited by using a CFC task. The fear behavior that animals display in such tasks follows a specific linear pattern where the emergence of the next set of behavior is determined by emotional intensity

and imminence according to the imminence-cascade model. Understanding these behaviors can help interpret fear behavior as this is used to study the neurological underpinnings of psychiatric disorders.

1.4 The Influence of Context on Fear Behavior

Previously, it was explained how, according to the defense-cascade model, the size of the response to a fearful situation depends on the emotional intensity of the threat. Different environmental factors can influence emotional intensity, and with that, fear behavior. For example, the emotional intensity of a rapidly approaching lion is lower when a fence is present between the lion and the person. The emotional intensity would also, for example, be different when there is a place to hide. Here, different environmental factors that can influence fear behavior will be explored.

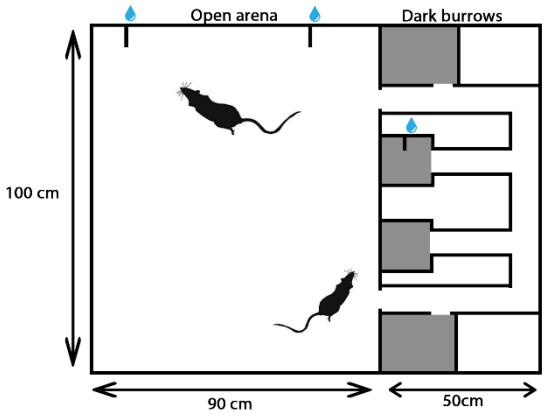

Figure 4. Visible burrow system (Taken from de Boer, 2021)

Environmental and contextual cues are important for determining which defensive behavior should be employed because cues provide information about the imminence of the threat and the environmental constraints of a situation (Rosen et al., 2008). For example, when exposed to a signal of danger, rats prefer to not freeze in the center, but they will first try to find cover by running toward a wall and start to freeze there (Kelley, 1985). However, when there is an opportunity to hide, for example by providing a burrow (Figure 4), they will most likely flee into the enclosed burrow (Blanchard & Blanchard, 1989; de Orca et al., 2007). Not only the presence of a hiding place influences fear behavior, but also environmental shape is a factor. One study compares the percentage of freezing that animals display in a square or elongated environment after being shocked in either a square or elongated environment (Figure 5). They show that animals who are shocked and tested in a square box freeze more than animals who are shocked and tested in an elongated box (Bolles & Collier, 1976). This shows that environmental shape is a factor that animals take into consideration when trying to cope with a fearful situation. Environmental size can also greatly influence fear behavior. A study by Rozen et al. (2008) exposes rats to trimethylthiazoline (TMT) in differently sized environments. TMT is a fear-inducing synthetic compound that is originally extracted from the feces of a fox, a natural predator of rodents (Vernet-Maury et al., 1984). The study looks at the freezing percentage of animals who are exposed to TMT in a small, medium, or large environment and found a big effect of environmental size on freezing as the animals show significantly less freezing behavior in larger chambers (Figure 6).

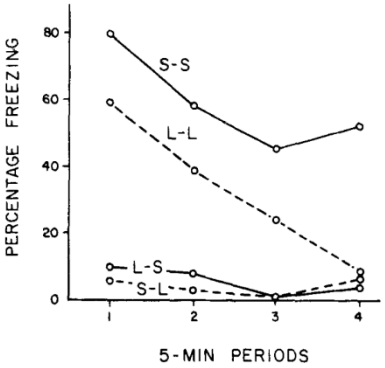

Figure 5. Freezing percentage in a long box L or a square box S after first being shocked in either L or S (Taken from Bolles & Collier, 1976)

Overall, fear behaviors such as freezing can be very useful to study the core mechanisms of psychiatric disorders and environmental context can be a very important factor for these kinds of behaviors. Factors such as environmental shape and size can greatly influence freezing behavior. By knowing which features play a role in fear behavior and by manipulating these features, researchers can gain valuable insights into the mechanisms underlying fear behavior, which in turn can enhance our understanding of psychiatric disorders.

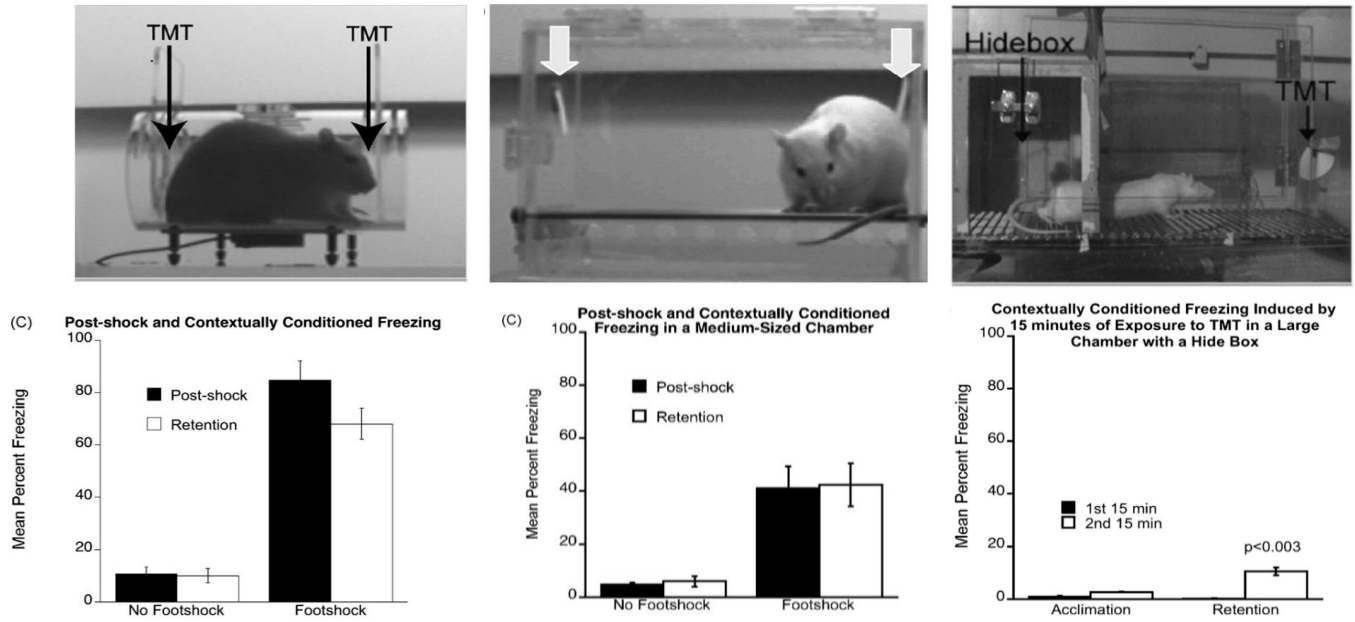

Figure 6. Freezing behavior of rats exposed to TMT in a small (a), medium (b) or large (c) environment (Taken from Rosen et al., 2008)

1.5 Delving into the Neurobiological Networks of the Fear Response

When negative emotions are experienced, for example during psychiatric disorders, neuronal fear networks are activated. This activation will elicit fear behavior but can also lead to an increased experience of negative emotions (Hinton et al., 2009). Diving deeper into the neuronal networks of fear behavior can be very insightful to fully understand what happens during negative experiences and psychiatric disorders.

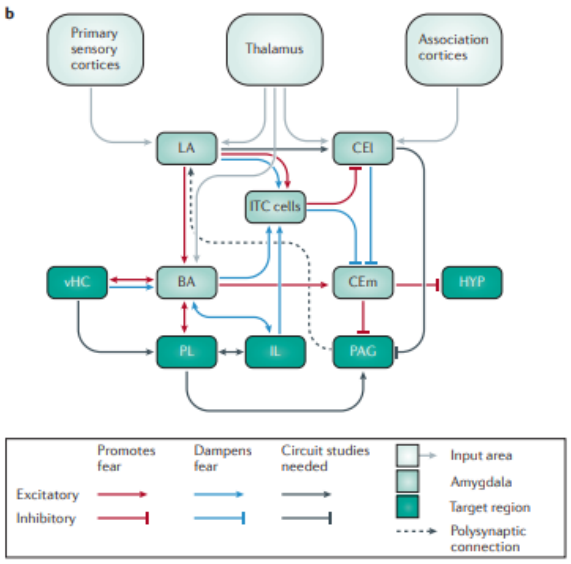

Figure 7. The fear and extinction network. Basal amygdala (BA), ventral hippocampus (vHC), prelimbic cortex (PL), infralimbic cortex (IL), intercalated (ITC), lateral central amygdala (CEl) nuclei, hypothalamus (HYP), periaqueductal grey (PAG), medial central amygdala (CEm), lateral amygdala (LA) (Taken from Tovote et al., 2015)

As defensive behavioral responses are extremely important for an animal's survival, there is a distributed network of brain regions that are involved in learning and expressing these fear responses (Figure 7). Fear memories recruit various brain regions and circuits. Input areas such as the primary sensory cortices, thalamus, and association cortices provide information to several nuclei of the amygdala and act as sites of fear-related neuronal plasticity (Tsvetkov et al., 2002; Bordi & LeDoux, 1994; Belova 2007). This plasticity is regulated by bidirectional connections between the basal amygdala (BA) and the ventral hippocampus (vHC), as well as between the BA and the prelimbic cortex (PL) (Felix-Ortiz et al., 2013; Senn et al., 2014). Afterwards, central nuclei of the amygdala project to regions such as the hypothalamus and periaqueductal gray to promote fear behavior (LeDouc et al., 1988; Tovote et al., 2016). Extinction of fear is mediated by other brain regions. To reduce the fear, output from the lateral central amygdala nuclei to the hypothalamus and periaqueductal gray, and input from that infralimbic cortex to the basal amygdala and the intercalated cells are important (Senn et al., 2014).

Overall, fear memories engage various brain circuits. These circuits represent a mechanism that allows the rapid and flexible selection of behavioral programs necessary for survival (Fadok et al., 2017). Understanding how these brain areas interact offers insights into fear processing and helps the further understanding of disorders that stem from dysregulation of the fear process. In the following chapters, the role of two vital brain areas will be explored: the lateral hypothalamus and the periaqueductal gray. By understanding their specific contributions to fear behavior, we aim to gain a deeper understanding of the underlying mechanisms driving fear behavior.

1.6 Fear and the Lateral Hypothalamus: Insights from Emerging Research

As previously discussed, the fear response brain network involves many brain areas and one of the output areas of the amygdala in this network is the hypothalamus. It is involved in both the initiation and extinction of fear behavior. Among the regions within the hypothalamus, the lateral hypothalamus (LHA) has emerged as a particularly significant area for fear behavior. In the following section, the diverse functions associated with the lateral hypothalamus (LHA) and its significant role in fear behavior will be explored, shedding light on its contributions to the mechanisms underlying fear processing.

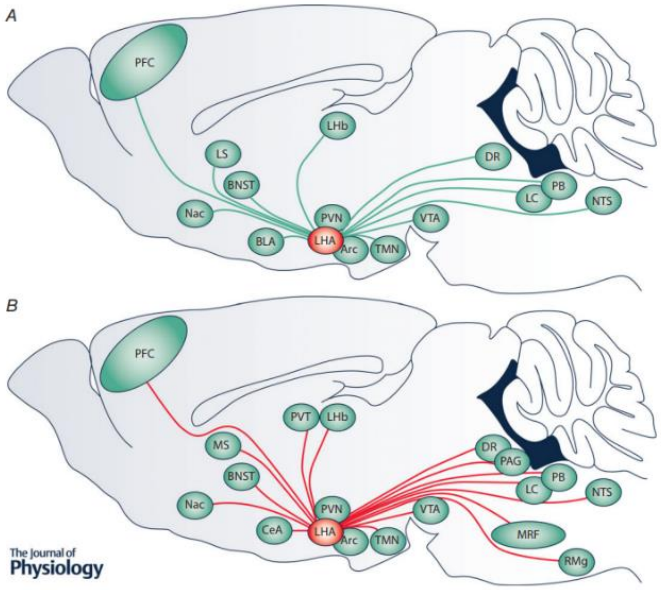

Figure 8. Brain-wide connections of the LHA A) Major long-range inputs (green lines) to the LHA. B Major long-range outputs (yellow lines) from the LHA. Arc, arcuate nucleus; BLA, basolateral amygdala; BNST, bed nucleus of the stria terminalis; CeA, central nucleus of the amygdala; DR, dorsal raphe; Fx, fornix; LC, locus coeruleus; LHA, lateral hypothalamic area; LHb, lateral habenula; LS, lateral sulcus; MRF, midbrain reticular formation; MT, mammalothalamic tract; NAc, nucleus accumbens; NTS, nucleus of the solitary tract; PAG, periaqueductal gray; PB, peribrachial brainstem; PFC, prefrontal cortex; PVN, paraventricular nucleus of the hypothalamus; PVT, paraventricular nucleus of the thalamus; RMg, nucleus raphe magnus; TMN, tuberomamillary nucleus; VTA, ventral tegmental area (Taken from Bonnavion et al., 2016)

The LHA is a functionally discrete structure within the hypothalamus that regulates functions such as feeding, arousal, energy balance, stress, motivated behavior, and reward (Berthoud & Münzberg, 2011; Burdakov et al., 2013; Hurley & Johnson, 2014; Brown et al., 2015; Stuber & Wise, 2016). Because the LHA is involved in a wide range of behaviors, it is unsurprising that it is highly connected to many different brain regions (Figure 8). The LHA is comprised of an intricate assembly of cell types and circuits with unique patterns of inputs and outputs that interconnect with different physiological systems (Geeraedts et al., 1990; Bernardis & Bellinger, 1993; Swanson et al., 2005; Hahn & Swanson, 2010). The LHA acts as a hub for the integration of diverse central and peripheral signals and coordinates adaptive behavioral responses to the environment (Reviewed by Bonnavion et al., 2016).

Other than orchestrating food and motivated behavior, the LHA is also important for stress and anxiety behavior. The LHA is highly interconnected with the PAG, amygdala, and habenula; all of which are important for defensive behaviors (Hahn et al., 2015; Brandão et al., 2008; Pobbe & Zangrossi, 2010). One study has directly investigated the effect of activating and silencing the LHA on defensive behavior, however this study was a Master's thesis and not a peer reviewed article. This thesis shows that optogenetically activating the LHA is sufficient to elicit freezing behavior. Additionally, their data shows that DREADD silencing of the LHA during contextual fear memory does not influence freezing. However, they have found an effect of the DREADD silencing response to a looming shadow stimulus. From this, they conclude that LHA activity is necessary for innate fear and not learned fear (Tully, 2015). Specifically, the hypocretin/orexin (Hcr/Ox) system of the LHA is very important for stress, anxiety, and other high-arousal states (Johnson et al., 2012; Giardino & de Lecea,

2014). This is apparent as increased Hcr/OX neuronal activity is measured during immobilization stress (González et al., 2016). These neurons are found to be necessary for freezing behavior as Hcrt-1 receptor knockout mice show an impaired freezing response and reduced neuronal activation in the lateral amygdala (Figure 9.) (Soya et al., 2013). Additionally, activating these neurons leads to increased stress. In vivo, optogenetic activation of Hcrt/Ox causes increased hypothalamic–pituitary–adrenal axis activity, which is the principal effector of the stress response. Additionally, the animals also showed freezing-like behaviors, further proving that the LHA has a role in fear behavior (Bonnavion et al., 2015).

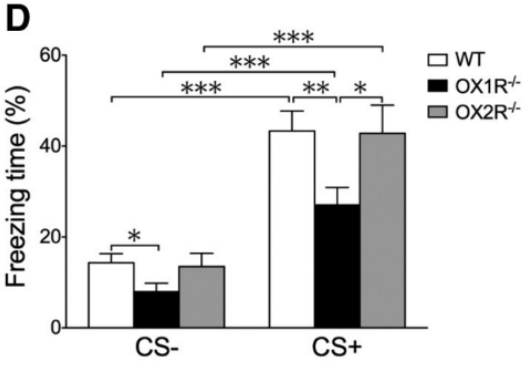

Figure 9. Freezing behavior of wildtype (WT), Ox1r-/-mice and Ox2r-/- mice in cued fear-conditioning tests (Taken from Soya et al., 2013)

Overall, the LHA is one of many regions important for or orchestrating defensive behavior. Specifically, the Hcrt/Ox neurons seem to be important mediators for this behavior. Investigating this area further could be an interesting approach to learn more about how defensive behavior is orchestrated in the brain.

1.7 The Periaqueductal Gray's Role in Fearful Encounters

As mentioned earlier, the fear response network encompasses a vast array of brain regions with multiple important output regions. Next to the LHA, the periaqueductal gray (PAG) has long been recognized as a central player in defensive behaviors, with a wealth of research highlighting its crucial role. In the following section, PAG's involvement in fear behavior will be explored to further unravel the complex neurobiology underlying fear.

The PAG is a dense region surrounding the midbrain aqueduct that is known for its essential role in defensive behavior (Fanselow 1991, Fanselow 1994, Deng et al., 2016). It is an anatomic and functional interface between the forebrain and the lower brainstem and has a major role in coordinating behavioral responses to internal stressors such as pain and external stressors such as threats (Cheriyan & Sheets, 2018; McNaughton & Corr, 2004). It is made up of distinct columns that receive selective inputs from the prefrontal cortex, amygdala, hypothalamus, and nociceptive pathways and it coordinates specific patterns of cardiovascular, respiratory, motor, and pain modulatory responses (Figure 10) (reviewed by Benarroch, 2012).

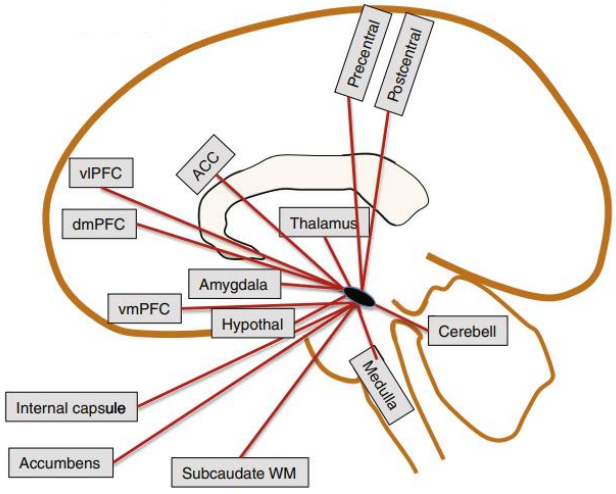

Figure 10. PAG connections. ACC = anterior cingulate cortex, Cerebell = cerebellum, dmPFC = dorsomedial prefrontal cortex, vmPFC = ventromedial prefrontal cortex, vlPFC = ventrolateral prefrontal cortex, WM = white matter. (Taken from Linnman et al., 2012)

The PAG is essential for the organization of the response to external threats, such as predators. It is suspected to be an essential part of the neurocircuitry that produces fleeing or freezing responses to threats (Tovote et al. 2016). It receives input from essential forebrain areas that regulate defensive behavior such as the central nucleus of the amygdala (CEA), the hypothalamus, and the medial prefrontal cortex (Rizvi et al., 1991; Wang et al., 2015; An et al., 1998). The importance of the PAG in defensive behavior is shown by lesions of the PAG as they impair the fear responses that are normally brought on by activation of the amygdala or hypothalamus (Hunsperger, 1963). On the other side,

stimulation of the PAG is sufficient to induce various defensive responses including freezing and escape (Silva et al. 2013).

Overall, the PAG is an important brain region with an essential role in defensive behavior as it is both necessary and sufficient for fear behavior. Because this is such a well-studied brain region regarding fear behavior, is it also an interesting area to investigate in new studies as new parameters or experimental setups can provide even more information about how fear behavior is organized.

1.8 Memory plays a part in fear behavior

Previously, the intricate network underlying fear behavior and a few important brain regions were explored. However, although immediate stimuli, context, and the activity of brain regions in response to these factors are crucial for defensive behavior; it also heavily relies on memory. In this chapter, we will shed light on how memory and fear shape behavioral outcomes.

When an animal is confronted with a threat, it has to employ an appropriate defensive response based on previous experiences and weigh cues and contextual information that could predict danger or safety. Because aversive experiences are not identical, to be able to apply past fearful experiences to future encounters, memory generalization is needed (Asok et al., 2019). Generalization can be influenced by different factors, such as the intensity of a negative experience (Figure 11), early-life stress, and the saliency of elements in the environment (Baldi et al., 2004; Elliott and Richardson, 2018; Huckleberry et al., 2016). Because appropriate fear responses are vital in nature and generalization depends on memory, proper generalization is just as vital. Not only, is it found that generalization is important for fear behavior, over-generalization has been found to be a major feature of anxiety- and stress-related disorders such as posttraumatic stress disorder (Elzinga & Bremner, 2002). This solidifies the importance of understanding how memory works to be able to research fear behavior to be able to learn more about the underpinnings of neuropsychiatric disorders.

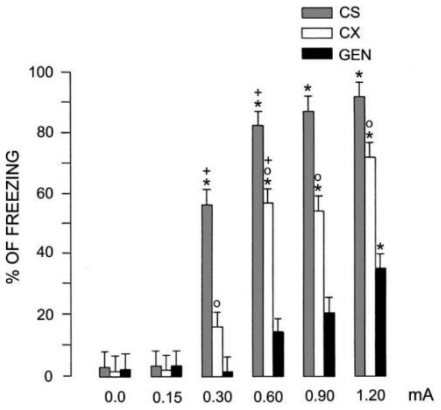

Figure 11. Footshock intensity and fear conditioning in the conditioning context (CX), acoustic CS in diverse context (CS) and diverse context before CS presentation (generalization phenomenon) (GEN) (Taken from Baldi et al., 2004).

There are different forms of memory: long-term and short-term memory. Short term memory (STM) is a capacity-limited system that holds information that is no longer being actively perceived (Posner, 1980). Long-term memory can last days to weeks and sometimes, even a lifetime (Bailey et al., 1996). Memory consolidation is the process where a temporary memory is transformed into a more stable permanent memory (Müller & Pilzecker, 1900; Lechner et al., 1999). This stable memory is referred to as a memory trace or memory engram (Thompson, 2005; Semon, 1911). During an experience, information will be combined into a cohesive event that contains information about what occurred, where, and when, in a form that is freely available to recall at a later time. This is called episodic memory (reviewed by Tonegawa et al., 2018). The hippocampus (HC) is a brain area that plays a central role in the formation of episodic memory within the mammalian brain (Scoville & Milner, 1957, Squire et al., 1992; Aggleton &

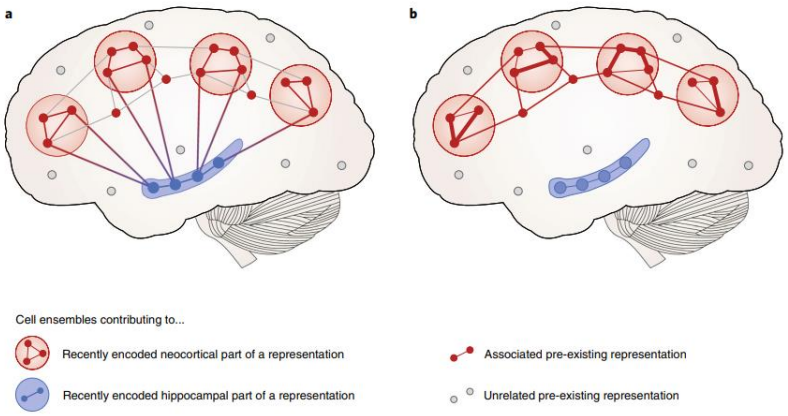

Figure 12. Memory reactivations strengthen neocortical representations. A) A newly encoded representation of an experience. B) Repeated reactivations result in a systems-level reorganization of the representation (Taken from Klinzing et al., 2019)

Brown, 1999; reviewed by Eichenbaum (2000)). Through the process of memory consolidation, repetitive reactivation of these hippocampal neurons strengthens the memory representations in the neocortex (Diekelmann & Born, 2010). Over time, the slowly learning neocortex integrates these strengthened representations into pre-existing long-term memories (Figure 12) (Kumaran et al., 2016).

As previously mentioned, the HC is the central region for the formation of episodic memory. This vital role of the HC for memory functioning is further shown by lesion and activation studies. In one study, animals are trained in a water maze to find a hidden platform (Morris, 1984). Afterwards, the animals' HC is lesioned, and the data demonstrates that none of the lesion groups show evidence of memory, as the detection of the platform occurs at chance level time. (Figure 13). This shows that spatial memory is disrupted when the HC is lesioned (Clark et al., 2005). Furthermore, it was shown that hippocampal activation in patients with mild cognitive impairment was necessary for successful memory encoding (Kircher et al., 2007).

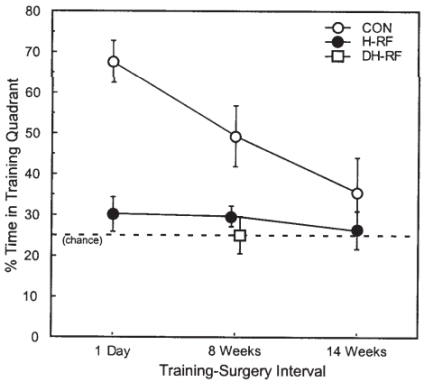

Figure 13. Water maze performance of control animals (CON), animals with a complete hippocampal lesion (H-RF) and rats with a dorsal hippocampal lesion (DH-RF) (Taken from Clark et al., 2005)

Not only is the HC very important for memory, but it also has a crucial role in defensive behavior. This connection might not be very surprising as, as explained before, memory is very important for defensive behavior and the HC is very important for memory. A study by Richmond et al. (1999) shows the importance of the HC for defensive behavior by lesioning the HC and revealing that contextual freezing is impaired after CFC. A difference is found between the dorsal and ventral HC as lesioning the dorsal HC does not affect conditioned defensive behavior while lesioning the ventral HC does decrease conditioned defensive behaviors (Pentkowski et al., 2006; Trivedi et al., 2004). Furthermore, the effect of dorsal and ventral ibotenic acid lesions of the HC in male Long-Evans hooded rats exposed to cat odor on unconditioned defensive behaviors is also studied. This study shows that ventral hippocampal lesions reduce unconditioned defensive behavior while dorsal hippocampal lesions do not alter any defensive behaviors (Pentokowski et al., 2006).

Overall, memory is essential for defensive behavior because the response to a threat is based on previous experiences. Additionally, the HC is an area that is very important for memory and defensive behaviors. That HC lesioning is detrimental to defensive behavior demonstrates the importance of memory in defensive behavior because it shows that when memory function is impaired, defensive behavior is also disturbed.

1.9 Engram Cells: The Hidden Architects of Memory

The findings that proper HC functioning is essential for both memory and defensive behavior show that memory and defensive behavior are strongly interconnected, and that the HC is a vital region for the functioning of both. Coincidentally, in a paper by Liu & Ramirez et al. (2012), a sparse but specific ensemble of hippocampal neurons has been found that contribute to a memory engram. The discovery of this neurological representation of memory has helped the understanding of the mechanisms underlying memory formation and retrieval. The term 'engram,' first used by R. Semon, refers to the neural substrate for storing and recalling memories and is essentially equivalent to a ‘memory trace’ (Semon, 1925; Schacter, 1982; Schacter et al., 1978). Recent studies show that memory is encoded by sporadically distributed populations of neurons that are highly activated during learning (Whitaker and Hope, 2018; Josselyn and Tonegawa, 2020). These neurons undergo physical and/or chemical changes and can be selectively reactivated to produce the retrieval of the experience or inhibited to prevent the retrieval of the experience (Tonegawa et al., 2015; Josselyn et al., 2015). The changes that these cells undergo include synaptic plasticity (including LTP and LTD), enhanced excitability of whole single cells, transient activation of immediate early genes (IEGs), new rounds of

protein synthesis, and structural changes of dendritic spines which include growth and contraction. When the stored information is available, the engram can be re-excited for recall (Figure 14) (Liu et al., 2014). The discovery of these cells gave concrete evidence for an engram associated with a specific memory in the brain (Tonegawa et al., 2018; Semon, 1911).

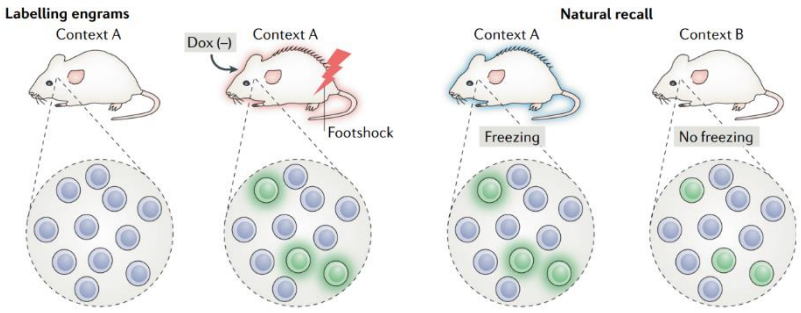

Figure 14. Engram activation during engram labelling and natural recall in the same or a different context (Adapted from Tonegawa et al., 2018)

An engram can be defined by three criteria: 1) the engram goes through physical and/or chemical change that occurs in the neural network, 2) this change is a result of the activation of neuronal subpopulations by episodic stimuli, and 3) it can be subsequently reactivated by stimuli that were part of the original set of encoded stimuli, resulting in the recall of the original memory (Thompson, 2005; Tonegawa et al., 2015; Josselyn et al., 2015). Recent developments in techniques allow the identification of engram cells for a particular memory. Specifically, the engram identified in the hippocampal dentate gyrus granule cells for contextual fear memory meets all three of the criteria (Liu et al., 2012).

Multiple studies show that selective ablation or inhibition of neurons that correlate to a memory engram erases fear memory responses (Han et al., 2009; Zhou et al., 2009). However, if you want to prove that specific cells are the cellular basis of a specific fear memory engram, you need to show that direct activation of these cells will induce the specific behavioral output that is associated with these cells (Martin et al., 2002; Gerber et al., 2004). Because of this, Liu and Ramirez et al. (2012) target the DG of c-Fos-tTA transgenic mice with the AAV9-TRE-ChR2-EYFP virus and an optical fiber implant to specifically activate DG engram cells that were activated during CFC. They show that delivering blue light pulses, increases spike probability precisely time-locked to the onset of light pulses. Next to this, this optical activation of ChR2-EYFP-positive DG cells causes light-induced freezing (Figure 15).

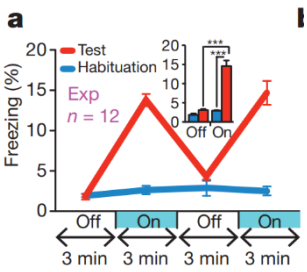

Figure 15. Optical stimulation of engram-bearing cells induces post training freezing (Taken from Liu & Ramirez et al., 2012)

This finding has led to a variety of new papers that have test the boundaries of memory formation and retrieval by changing memories or inducing fake ones. For example, internal representations of a fear memory can be combined with external stimuli to create a new memory. Researchers induce this fake memory in the HC by activating pre-existing contextual memory engram-bearing cells with a neutral emotional valence in a new environment while simultaneously delivering foot shock. Afterwards, animals begin to freeze in this originally neutral context, showing that a fake memory is created (Ramirez et al., 2013). Additionally, one study switches the valence of a memory. First, they label active cells during contextual or reward conditioning. Then, they activate these cells while subjecting the animals to a second conditioning of the opposite valence. Lastly, they examine place preference or avoidance and see behavior that signal that the valence of their memory is switched (Redondo et al., 2014). One study shows that a false memory can be created without the presence of an experience. This is possible by pairing a foot shock with the activation of a specific olfactory glomerulus that

corresponds to a specific odor that the animals have not experienced before. Afterwards, the animals avoid this odor, which they have never smelled before, showing that a new memory is created (Vetere et al., 2017).

By looking further into these memory engram-bearing cells, the mechanisms of memory formation and consolidation in healthy but also animals that exhibit pathological conditions can be investigated. For example, engram research has given more insights into the mechanisms of memory consolidation. One study investigates the neural circuit mechanisms underlying the formation and maturation of neocortical memories and finds that neocortical prefrontal memory engram cells rapidly generate during learning. At first, they are immature and silent but become functionally mature and retrievable over time with support from HC memory engram cells. Whereas the HC engram cells become gradually silent over time (Kitamura et al., 2017). As said before, investigating memory engram-bearing cells can also be used to study memory in animals that exhibit pathological conditions. One study induces retrograde amnesia by using protein synthesis inhibitors to disrupt memory consolidation. They find that synaptic strength and dendritic spine density increases in consolidated memory engram cells, but not in engram cells that are amnesiac because of the protein synthesis inhibitor. However, memory retrieval can be induced in these animals by optogenetic activation of these cells which also correlates with retained engram cell-specific connectivity (Figure 16). This suggests that the strengthened synapses in engram cells are critical for memory retrieval and that a specific pattern of connectivity of engram cells is crucial for memory storage (Ryan et al., 2015).

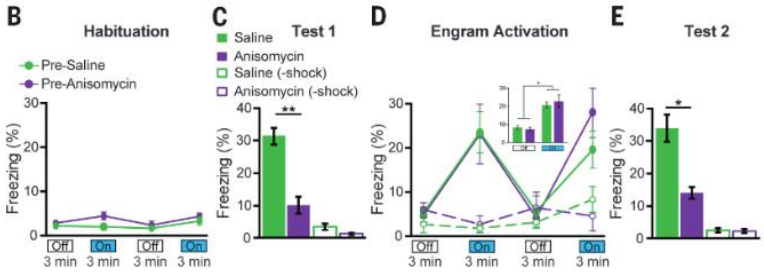

Figure 16. Optogenetic stimulation of engram cells restores fear memory in retrograde amnesia. (B) habituation to context A. (C) memory recall in context B 1 day after testing. (D) memory recall in context A 2 days after engram activation training. (E) memory recall in context B 3 days after engram activation training (Taken from Ryan et al., 2015)

Overall, the discovery of engram cells helps further unravel the underpinnings of memory. Recent research demonstrates that memories are not fixed entities but are malleable and subject to change. It is revealed that not only can existing memories be modified, but entirely new memories can be artificially induced. This newfound understanding opens a world of possibilities for studying memory processes in both healthy and unhealthy animals. By investigating the engram cells and their functioning in various contexts, researchers can gain valuable insights into the mechanisms underlying memory formation, retrieval, and alteration. As said before, memory dysregulation, such as over-generalization, is seen in individuals who suffer from psychiatric disorders. As fear behavior and memory are both highly connected, examining fear engrams can be a useful tool to help further the knowledge of disorders where this fear memory is not properly managed.

1.10 Research questions

Gaining more mechanistic insight into the neuronal circuits that are involved in fear memory and defensive behaviors can help gain more insights into treating cognitive disorders that involve memory. Because of this, we wanted to investigate the neuronal circuits that are involved in fear memory and defensive behaviors, and how a fear engram influences both brain and behavior states. We did this by perturbation and observation of two downstream brain areas of the HC.

Based on previously unpublished research by Dorst & Senne et al. it is discovered that the lateral hypothalamus is an important brain area for fear memory engram reactivation and therefore one of our aims was to examine the effect of the perturbation of this area during fear engram activation. The main question for this part of the research is: 'What is the effect of chemogenetic inhibition of the lateral hypothalamus during fear memory engram reactivation on freezing behavior and cFos expression?'. We hypothesized that, because of its importance for fear behavior, chemogenetic inhibition of the lateral hypothalamus will decrease freezing behavior. Furthermore, we hypothesized that because the area is inhibited, cFos expression will also decrease.

Next to the perturbation of an area, we also wanted to observe the neuronal activity of a downstream brain area of the HC. Because of its well-described role in fear and freezing behavior, we chose to observe the neuronal activity of the PAG using fiber photometry. The main question for this part of the research is: 'What is the effect of optogenetic stimulation of fear memory engrams in differently sized environments on freezing behavior and PAG neuronal activity'. It is known that optogenetically activating a fear memory engram induces freezing and based on the previous findings of Rosen et al. (2008), we hypothesized that animals would freeze more in smaller environments when their fear memory engram cells are optogenetically activated. Furthermore, because of its well-established role in freezing in literature, we hypothesized that when animals are freezing, neuronal activity of the PAG will be higher. Because the PAG is involved in freezing behavior, we hypothesized that the neuronal activity within the PAG will be higher during the display of this behavior. Furthermore, because it is known that optogenetically activating a fear memory engram induces freezing, we hypothesized that optogenetically activating a fear memory engram will increase PAG neuronal activity.

2. Methods

2.1 Animals

For the experiments, 12 wildtype male C57BL/6 mice were used for the chemogenetics experiment, and 6 wildtype male C57BL/6 mice were used for the fiber photometry experiment. These mice were acquired from the Charles River Laboratories and were 2-3 months of age. The mice were housed in groups of 3-4 mice per cage. When necessary, aggressor mice were separated from cage mates and were singly housed with extra enrichment. The animals were on a 12:12 light-dark cycle (07:00 – 19:00) in humidity-controlled colony rooms with *ad libitum* access to standard rodent chow and water. After their arrival at the facility, the mice were not handled for three days. 24 hours before surgery, the standard rodent chow was substituted with 40 mg/kg doxycycline (DOX) chow. Animals were left undisturbed for ten days after surgery to facilitate recovery. A scheme with the timelines of the whole experiments of both the LHA chemogenetic inhibition groups and the PAG fiber photometry groups can be found in Figure 17 and Figure 18.

Four days before surgery, the chemogenetic mice were wheel trained to make sure data is comparable to previous studies. Two custom-built apparatuses (13 cm L x 13 cm W x 31 cm H) were built and equipped with a 12-inch horizontal wheel that is connected to an axis linked to an Arduino. Aggregate axel data (e.g., number of rotations, time rotating, number of pulses) was collected through a custom MATLAB script.

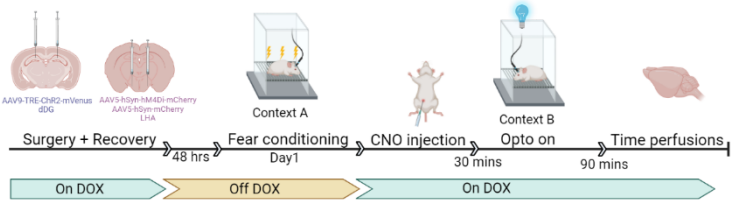

Figure 17. Timeline of the LHA chemogenetic experiment

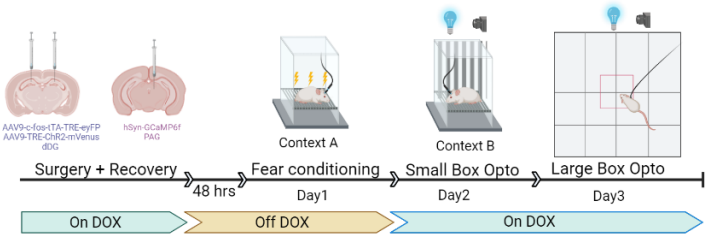

Figure 18. Timeline of the PAG fiber photometry experiment

2.2 Surgeries

The protocol for the implant surgeries for the PAG fiber photometry experiment and LHA chemogenetic experiment be found in Appendix 6.1. For the surgeries for both the PAG fiber photometry observation and LHA chemogenetic inhibition animals, the mice were weighed and placed into an induction chamber that was filled with a blend of 70% oxygen and 4% isoflurane for anesthetization. Afterwards, the mice were mounted in the nosecone of the stereotaxic frame (Kopf Instruments, Tujunga, CA, USA) and the anesthesia was maintained with a 2% isoflurane and 70% oxygen mixture. Ophthalmic ointment was applied to both eyeballs to prevent them from drying out and hair was removed by topically applying hair removal cream. The scalp was cleaned with ethanol and betadine and 2% lidocaine (Clipper Distributing Company) was applied topically to the surface for topical analgesia. An incision was made to expose the skull and to bleach the skull structures, peroxide was applied to the surface of the skull. After this, the skull was leveled between bregma and lambda.

The LHA chemogenetic inhibition mice were injected bilaterally in two different brain regions: the dorsal dentate gyrus (dDG) and the lateral hypothalamus (LHA) (Figure 19). The injection coordinates were in relation to bregma (in mm): for dDG: AP = -2.2, ML = ±1.3, DV = -2.0; for the LHA: AP = -1.3, ML = ±1.25, DV = -5.3. Different viruses were used for the two different brain areas; one for the activity-dependent 'tagging' (see Tet-Tag system) and one for the chemogenetic manipulations (see Chemogenetics). The dDG was injected with the two viruses for the

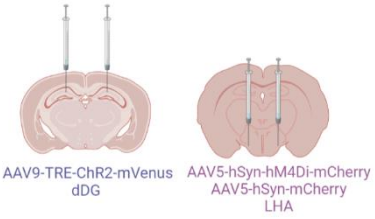

Figure 19. Viral injections in the dDG and LHA for chemogenetic inhibition animals

activity-dependent ‘tagging’ system. These were packaged at the University of Massachusetts Amherst Viral Vector Core. The first is a virus that contains a pAAV-cFos-tTA plasmid vector and the second contains an pAAV-TRE-chR2-eYFP for ‘tagging’. The LHA was injected with either an AAV5-hSyn-hM4D(Gi)-mCherry viral construct (Addgene viral prep 50467-AAV5) for the chemogenic inhibition or with AAV5-hSyn-mCherry (Addgene viral prep 114472-AAV5) for the control group.

The PAG fiber photometry mice were also injected bilaterally in the dDG but unilaterally in the PAG (Figure 20). The injection coordinates were in relation to bregma (in mm): for the dDG: AP = -2.2, ML = ±1.3, DV = -2.0; for the PAG: AP = -4.45, ML = -0.5, DV = -2.5 and DV = -2.7. Different viruses were used for the two different brain areas one for the activity-dependent ‘tagging’ and one for the fiber photometry. The dDG was injected with the two viruses for the activity-dependent ‘tagging’ system. These were packaged at the University of Massachusetts Amherst Viral Vector Core. The first is a virus that contains a pAAV9-cFos-tTA plasmid vector and the second contains a pAAV-TRE-chR2-eYFP for ‘tagging’ or a pAAV-TRE-eYFP for control experiments. The PAG was injected with an AAV9-Syn-GCaMP6f viral construct (Addgene viral prep 100837-AAV9).

For the viral injections, bilateral craniotomies were made above the injection sites. For all injections, A 33-gauge beveled needle that was connected to a 10 µl Hamilton syringe was attached to a micro-infusion pump (UMP3, World Precision Instruments) was used for the viral injections. First, the needle was lowered 0.2 mm past the injection site and was kept stationary for 2 minutes. Then, the needle was raised to the site of injection and after another waiting period of 1 minute, the virus injection occurred. In the dDG, 200 nl of virus was injected at a rate of 110 nl/min, in the LHA, 300 nl of the virus was injected at a rate of 110 nl/min, and in the PAG, for both injections, 200 nl of virus was injected at a rate of 40 nl/min. The injection was followed by a 5-minute wait period. Afterwards, the needle was raised 0.2mm above the injection site and was left stationary for 3 minutes before completely raising up and removing the needle.

After injections, all mice were implanted with bilateral fiber optics (200 µm core diameter; Doric Lenses) directly above the site of viral injections at -1.8 DV. Furthermore, for the chemogenetic mice, skull screws were anchored to help secure the implants. The implants and skull screws were sealed by a head cap that was a buildup of layers of metabond and dental cement (A-M systems). For the PAG fiber photometry mice, a unilateral optic fiber (200 µm core diameter) was implanted at the site of injection at -2.6 DV. This implant was secured to the skull with a layer of adhesive cement and multiple layers of dental cement.

After surgery, the mice received a 0.1 ml intraperitoneal injection of 0.3 mg/ml buprenorphine, and a subcutaneous 0.5 mg/ml injection of meloxicam, and a 0.2 ml subcutaneous injection of saline and were placed on a heating pad until conscious recovery.

2.3 Tet-Tag system

A common way to study fear memory is by exposing a rodent to fear by tagging/labeling the fear engram by exposing them to a fear-inducing stimulus such as a shock in the CFC paradigm and afterwards activating the fear engram with optogenetics.

Tagging the fear engram and reactivating it with optogenetics is mostly done by targeting specific brain areas of cFos-tTA transgenic mice with an AAV9-TRE-ChR2-EYFP virus and an optical fiber implant (Figure 20) (Reijmers et al., 2007; Liu et al., 2012). This approach makes use of the cFos and the tetracycline transactivator (tTA). cFos is an immediate early gene that is often used as the marker of recent neuronal activity (Kubik et al., 2007). tTA is a key component of the doxycycline (DOX) system for the inducible

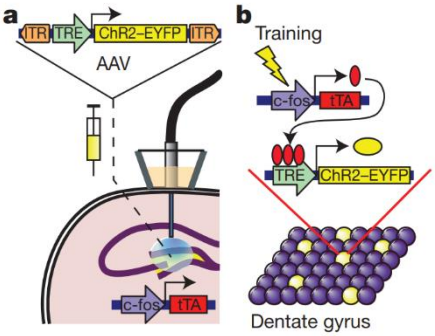

Figure 20. tTA-TRE activity driven selective labelling of DG cells by ChR2-eYFP during an experience (Taken from Liu & Ramirez et al., 2012)

expression of a gene of interest (Shockett & Schatz, 1996). This uses tetracycline (tet) to regulate gene expression. In the presence of tet, a conformational change in the tet repressor prevents tTA from binding to its operator which stops the expression (Hinrichs et al., 1994). Two tet derivatives are Dox and anhydrotetracycline (Schockett & Schatz, 1996). When there is Dox present, the cFos-promoter-driven tTA cannot bind to its target tetracycline-responsive element (TRE) which means there is no expression. When Dox is absent, neuronal activity causes the release of cFos which causes the cFos-promoter-driven tTA to bind to the TRE site which causes the expression of ChR2-EYFP (enhanced yellow fluorescent protein). This expression of ChR2-EYFP allows the reactivation of the tagged engram cells by light stimulation during texting (Liu et al., 2012).

2.4 Fear engram labeling

Before CFC and behavior testing, the LHA chemogenetic inhibition animals were handled for 5 days and injected intraperitoneally with 0.1 ml of saline to habituate them to these actions. The animals in the PAG fiber photometry group did not get habituated to intraperitoneal injections. Two days before CFC, the animals were placed in a new cage where the doxycycline (DOX) diet was swapped with rodent chow and the animals were left undisturbed.

For CFC, mice were placed in mouse conditioning chambers with Plexiglass walls and a grid floor (Coublourn Instruments, Whitehall, PA, USA). The dimensions of the conditioning chamber are 17.78 cm W x 17.78 cm D x 30.5 cm H. This grid floor was connected to a precision shocker through which the mice received a series of four 2-second foot shocks with a 0.5mA intensity during an 8-minute tagging session. Because of the absence of DOX during this experience, fear-induced neuronal activity selectively labels active cFos expressing neurons with ChR2-EYFP. These tagged neurons can be reactivated in a different context by light stimulation during testing (Liu et al., 2012).

Immediately after the shock session, the mice were put in a clean cage and where they were put back on the DOX diet. The mice stayed on this DOX diet for the remainder of the experiment. During CFC, an overhead camera (Computar) collected video data and interfaced with FreezeFrame (Actimetrics, Wilette, IL, USA). Through this FreezeFrame setup, both the foot shock delivery and simple freezing analyses were performed. Freezing was defined during the CFC task as bouts of 1.25 secs or longer with minimal changes in pixel luminance as defined by a number pixel threshold, N.

2.5 Optogenetics

As mentioned before, the tet-tag system can be used to label engram cells that are active during CFC in the absence of DOX. Later, the reactivation of these engram cells is performed by a technique called optogenetics.

Optogenetics is the combination of genetic and optical methods to inhibit or excite cells of living tissue and behaving animals (Deisseroth, 2011). It uses microbial opsins, a gene family with each gene encoding a light-sensitive protein that causes an electrical current across cellular membranes in response to light (Deisseroth, 2015). Channelrhodopsin (ChR2) is an example of such a light-sensitive protein (Nagel et al., 2002). To be able to use these light-sensitive proteins in neurons, recombinant viruses are used. A lentivirus that contained ChR2 is constructed and injected in cultured rat neurons. Afterwards, it is seen that ChR2 was expressed in the neurons and when blue light is directed at these neurons, depolarizing currents are induced (Boyden et al., 2005). After this first discovery more viral vectors have been found that were able to introduce opsin into rodent and primate neural tissues. For example, adeno-associated viral vectors (AAV) can be used (Haubensak et al., 2010).

This technique was also used to activate labeled engram cells in this thesis. First, all patch chords were tested to ensure that they generated 10 mW of power. The patch chords were connected to a 450 nm laser diode of Doric lenses and two fiber optic implants were plugged into these patch chords per animal. The animals were put into an environment and were allowed to explore freely for ten minutes. The optogenetic protocol was first two minutes without stimulation, followed by two light cycles. The

light cycles consisted of a 2-minute light-on (light-ON) period and a two-minute light-off (light-OFF) period. The light-on periods consisted of 10ms pulses of 20 Hz. After the last light-OFF period, the mice were unplugged from the patch cord and returned to their home cage. During these sessions, a camera was set up to film the animals in the environments.

For the optogenetic activation, the LHA chemogenetic inhibition animals were placed into a similar condition chamber to the one that is used in the CFC paradigm, but in a neutral context (Context B) that they have not been in before. All PAG fiber photometry animals were placed into two differently sized environments during the optogenetic activation. On day 2, they were put into a small environment, that had the same dimensions as the conditioning chamber (17.78 cm W x 17.78 cm D x 30.5 cm H) but had a striped insert in the back and was located in a neutral context. To make the small environment more distinct from the CFC chamber, a small weight boat with an almond odor was placed near the small environment. On day 3, the animals were optogenetically activated in the large environment. This was an open field arena with the dimensions 63 cm L x 63 cm D x 45.5 cm. For the LHA chemogenetic inhibition animals, it was chosen to only do optogenetic activation in the small environment because this is where previous research shows the most freezing behavior is seen compared to a middle-size and large environment (Dorst & Senne et al., unpublished).

2.6 Chemogenetics

Another method of influencing neuronal activity, used in this thesis, is chemogenetics. This technique is similar to optogenetics, in the sense that it is used to precisely manipulate neuronal systems in awake, behaving animals. This technique uses engineered receptors and biologically inert ligands to influence neuronal activity (reviewed by Campbell & Marchant, 2018). This ligand is often administered by a systemic injection or a micro infusion (Alexander et al., 2009). Because it is beneficial to use a receptor that is activated only by the ligand, new receptors are produced specifically for this purpose called Designer Receptors Exclusively Activated by Designer Drugs (DREADDs) (Armbruster et al., 2007). First, the DREADDs are introduced in neurons through viral vector-mediated transfection. For example, AAVs or lentiviruses can be used (Yu et al., 2018; Schoderboeck et al., 2018). Then, the animal is injected with the ligand that will bind to the DREADD which will cause the neuronal activity to be altered. Clozapine-N-oxide (CNO) is an example of a ligand that binds to these G protein-coupled receptors and causes downstream signaling with which it can alter neuronal activity (Armbruster et al., 2007).

To silence the lateral hypothalamus, an inhibitory designer receptor was used that could only be activated by the designer drugs, hM4Di, that was fused to the pan-neuronal hSyn reporter. The hM4Di drives inhibition of infected neurons when it is bound to CNO (National Institute of Health NIDA Drug Supply Program). All mice were intraperitoneally injected with saline for five days prior to tagging for acclimatization. A 0.6 mg/ml solution containing CNO was prepared in sterile saline and 0.5% dimethyl sulfoxide. On the day of the chemogenetic experiment, 30 minutes before the optogenetic manipulation, the animals were intraperitoneally injected with a 3mg/kg dose of the CNO solution.

2.7 Fiber photometry

Fiber photometry is a technique that measures bulk population-wide calcium dynamics (Gunaydin et al., 2014). This technique uses the release of Ca^{2+} that happens during depolarizing electrical signals which is essential for elementary forms of neuronal communication such as chemical synaptic transmission. This signaling is also obligatory for complex processes like the induction of memory and learning (Stosiek et al., 2003). It uses genetically encoded Ca2+ indicators such as GCaMP proteins to be able to record this release. GCaMP consists of circularly permuted green fluorescent protein (cpGFP)25, the calcium-binding protein calmodulin (CaM), and the CaM-interacting M13 peptide. Calcium binding to the M13 domain of Calmodulin (CaM) triggers conformational changes in the protein which results in increased brightness (Chen et al., 2013). Fiber photometry leverages this

increase in brightness to measure neuronal activity. Through time-correlated single photon counting-based fiber optics, the light that is emitted from fluorescent molecules in the brain can be recorded. These optical fibers are coupled to an excitation light and are implanted in the brain above the brain region of interest. First, excitation pulses are sent out of the probe. Then, the fluorescent signals of neuronal activity indicators return through the same optical fiber and are detected by a detector (Guo et al., 2015).

The fiber photometry protocol can be found in appendix 6.2. All animals of the PAG fiber photometry group were plugged into a 470-nm LED (Neurophotometrics; FP3002) that delivered an excitation wavelength of light to the GCaMP6f expressing PAG neurons. These neurons emitted a 530 nm signal which was collected via the same fiber. Isobestic signals that were calcium-independent were simultaneously collected by alternating excitation with 415-nm LED to separate the effect of movement, tissue autofluorescence, and photobleaching from actual changes in fluorescence. These excitation wavelengths were collected using Bonsai with a sampling rate of 28 Hz. The data was analyzed using an in-house pipeline in Python. The signals were normalized using the median and converted to a z-score to allow for a comparison of event amplitude (peak height expressed as % dF/F), frequency (Hz), total fluorescence (calculated as the area under the curve), and duration (measured in seconds as full-width half maximum). Statistical analysis was carried out using Python, and the results are reported as the Mean ± SEM.

2.8 Brain imaging and cell counting

After the final experiments, all mice were transcardially perfused. 90 minutes after the second light-ON period, the mice were taken out of their home cage and put into a container that contained isoflurane until deeply unconscious. Afterwards, they were pinned down and their thorax was opened to expose the heart and, PFA was run through the body by a pump. After the body was stiffened and therefore fixed, the head was decapitated, and the brain was extracted.

After perfusions, the brains were stored in 4% PFA for 48 hours before slicing. Using a Leica VT100s vibratome, the brain sections that contained the dDG and LHA were sliced into 50µm slices and collected in cold PBS. First, the slices were incubated at room temperature for two hours in a 1x PBS + 2% Triton (PBST) and 5% normal goat serum (NGS) on an orbital shaker from Amazon. Afterwards, the slices were transferred to wells that contained a primary antibody solution and were left incubating for 48 hours on an orbital shaker at 4°C. The primary antibodies were 1:1000 rabbit anti-c-Fos (SySy) and 1:5000 chicken anti-GFP (Invitrogen). After 48 hours, the slices were washed with PBST two times 20 minutes each and incubated with the secondary antibody solution. The secondary antibodies were 1:200 Alexa 555 anti-rabbit (Invitrogen) and 1:200 Alexa 488 anti-chicken (Invitrogen). After this second incubation time, the slices were washed again as previously described and mounted onto microscope slides (VWR International, LLC) Cell nuclei were counterstained with DAPI that was added to Vectashield HartSet Mounting Medium on a coverslip and left to dry overnight.

To examine cFos levels and to verify virus expression an LSM-800 confocal microscope equipped with a 20x objective lens from Zeiss was used. The protocol for the confocal microscope can be found in appendix 6.3. Each region of interest (ROI) image consisted of 20 slices in a z-stack with a step size of 1.54 µm. Furthermore, a single image of the ROI was created by tiling the slices with a 10% overlap. Images were either taken manually without a focus strategy, or they were automatically captured using the Software Autofocus feature in the Zen Blue software (version 2.3) to identify the most intense fluorescent pixels within the defined z-stack.

2.9 Image and video analysis

The images collected with the confocal microscope were used to determine cFos counts in the LHA by using Ilastik: an interactive machine-learning program for (bio)image analysis (Berg et al. 2019). In this program, several reference images were loaded and used to train the program to distinguish cells

from the background and count them. Cell counts were performed for the DAPI-stained cells, the cFos-expressing cells, and the DREADD-expressing cells.

Additionally, all the video files that were taken during all testing sessions were imported into the program ANY-Maze. This program allows for supervised automated analysis of freezing and it was used to get the total amount of time spent freezing for all animals. For the PAG fiber photometry animals, the program was also used to get data on freezing bout initiation and termination. This behavioral data was time-locked to the fiber photometry time series data analysis.

2.10 Statistical analysis

All statistical analyses for the behavioral experiments were done using both Python 3.10 and GraphPad Prism Version 9.0. The data is displayed in the figures as Mean ± SEM. The behavioral data was divided into 2-minute intervals, which corresponded to light-epochs (ON vs. OFF), and a repeated-measures one-way ANOVA was used to evaluate differences in behavior across light-epochs. Further statistical analysis (two-way ANOVA, Welch's t-test) and post hoc analyses (Tukey's HSD) were conducted as necessary.

For the $cFos^{+}$ cell count statistical analysis, a two-tailed unpaired t-test was performed. To analyze the event metrics acquired from the fiber photometry fluorescence data, Mann-Whitney tests were performed. A peri-event analysis was performed, but due to time restraints, no statistical analysis was performed on this data.

All statistical tests were performed with an alpha level of 0.05. The results of the statistical tests are reported in each figure legend, with * = $p < 0.05$, ** = $p < 0.01$, and *** = $p < 0.001$.

3. Results

To investigate the neuronal circuits that are involved in fear memory and defensive behaviors, and how a fear engram influences both brain and behavior states, we examined two sub questions; 'What is the effect of chemogenetic inhibition of the lateral hypothalamus during fear memory engram cell activation on freezing behavior and cFos levels?' and 'What is the effect of optogenetic stimulation of fear memory engrams in differently sized environments on freezing behavior and neuronal activity in the PAG?'. We analyzed the freezing behavior of all animals during CFC and optogenetic activation to see if the optogenetic activation influences freezing behavior. We also analyzed if there was a difference between freezing behavior in the small or large environment for the PAG fiber photometry animals. Additionally, for the LHA chemogenetic inhibition animals, we compared the $cFos^{+}$ cell counts between control and DREADD animals. Lastly, for the PAG fiber photometry animals, we tested the event matrixes between the eYFP and the ChR2 animals for differences and, while no statistical analysis was performed, the peri-event graphs of the fluorescence signal are shown.

3.1 Freezing behavior of the chemogenetic experiment group

To test the effect of DREADD silencing of the LHA on fear behavior, we examined the freezing behavior of both the DREADD and the control animals. We hypothesized that during CFC all animals would freeze more over time as they received shocks. We further hypothesized that light-induced freezing would be reduced for DREADD animals, while control animals would show typical light-induced freezing.

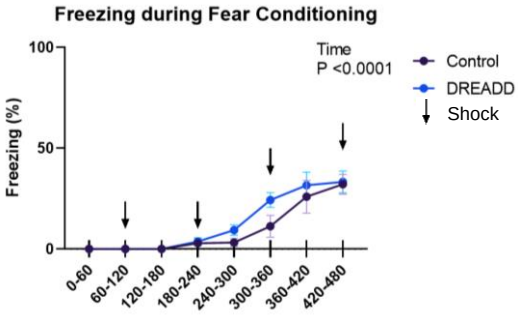

Figure 21. Freezing behavior (%) of control and DREADD animals during fear conditioning.

The freezing behavior of control and DREADD animals over time during fear conditioning can be seen in Figure 21. A two-way ANOVA analysis revealed that there is no significant effect of treatment on freezing behavior. However, there was a significant effect of time on freezing behavior (RM 2-way ANOVA; interaction: F (7, 70) = 0.9048, P=0.5079, Time: F (2.592, 25.92) = 30.36, P<0.0001, F (1, 10) = 1.725, P=0.2184).

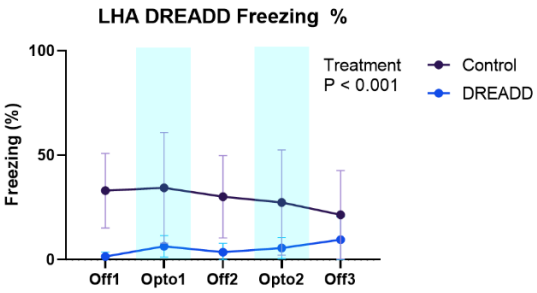

Figure 22. Freezing behavior (%) of control animals or animals who experienced chemogenetic inhibition of their LHA neurons.

The freezing behavior of the animals in the LHA chemogenetic inhibition experiment group across light epochs can be seen in Figure 22. It was found that DREADD animals exhibited near floor-levels of freezing. Statistical analysis showed that there was a significant effect of treatment on freezing percentage as DREADD animals spent significantly less time freezing than control animals. However, no difference in freezing was found for either group across light epochs (RM 2-way ANOVA; interaction: F (4, 40) = 1.402, P=0.2509, Time: F (4, 40) = 0.3322, P=0.8546, Treatment: F (1, 10) = 10.10, P=0.0098).

Overall, these results show that during CFC, the freezing behavior of both groups increases over time in a similar manner upon the reception of multiple shocks. Additionally, the freezing results show that the DREADD silencing of the LHA reduced freezing levels. Lastly, neither the control animals nor the DREADD animals show light-induced freezing.

3.2 cFos+ cell counts of the chemogenetic experiment group

To gain histological insight, we measured endogenous cFos expression in the LHA by the number of cFos$^+$ cells after optogenetic fear memory activation. We hypothesized that, because we were inhibiting the LHA, there would be less activity in this area and therefore also lower cFos expression and therefore fewer cFos$^+$ cells.

The percentage of cFos$^+$ cells of DAPI$^+$ cells in the LHA for control and DREADD chemogenetic inhibition animals can be seen in Figure 23. We analyzed if the percentage of cFos$^+$ of DAPI$^+$ cells in the LHA differed between control animals and animals whose LHA was chemogenetically inhibited by DREADDs. It was found that DREADD animals had a significantly higher percentage of cFos+ cells of DAPI+ cells (Unpaired t-test; t=5.039, df=96, P = <0.0001).

This shows that DREADD animals have a higher cFos expression in the LHA than control animals.

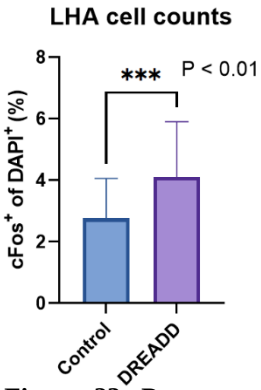

Figure 23. Percentage of cFos$^+$ cells of DAPI$^+$ cells for control and DREADD animals

3.3 Light-induced freezing behavior of animals in differently-sized environments

To test the effect of environmental size on fear behavior, we examined the freezing behavior of both eYFP and ChR2 PAG fiber photometry experimental animals in the small and large environments. We hypothesized that ChR2 animals would show light-induced freezing while eYFP animals would not. For the different environmental sizes, we hypothesized that ChR2 animals would freeze more during the light-on epochs in the small environment than in the large environment.

The freezing behavior of the animals in the PAG fiber photometry experiment group during CFC can be seen in Figure 24. A two-way ANOVA analysis revealed that there was no significant effect of treatment on freezing behavior. However, there was a significant effect of time on freezing behavior (RM 2-way ANOVA; interaction: F (8, 64) = 0.6227, P = 0.7557, Time: F (3.870, 30.96) = 51.23, P<0.0001, F (1, 8) = 0.08008, P=0.7844).

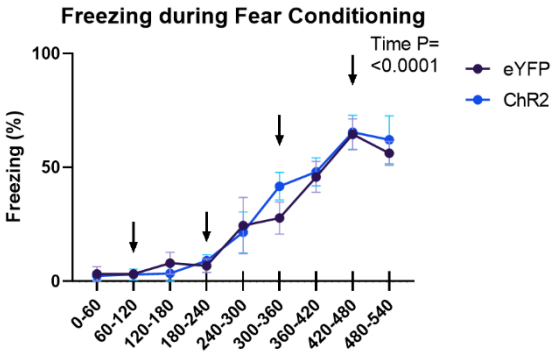

Figure 24. Freezing behavior (%) of control and DREADD animals during fear conditioning.

The freezing behavior of the animals in the PAG fiber photometry experiment group during optogenetic activation in the small box can be seen in Figure 25. There was no effect of optogenetic fear engram activation or treatment on freezing behavior in a small environment (RM 2-way ANOVA; interaction: F (4, 32) = 0.4139, P=0.7973, Time: F (1.963, 15.70) = 0.3445, P=0.7099, Treatment: F (1, 8) = 1.198, P=0.3055).

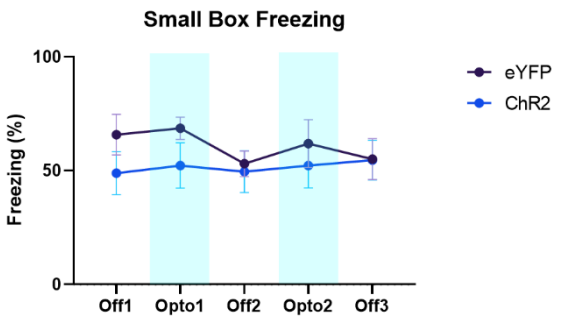

Figure 25. Freezing behavior (%) of control animals and animals who experienced optogenetic activation of a fear memory in a small box.

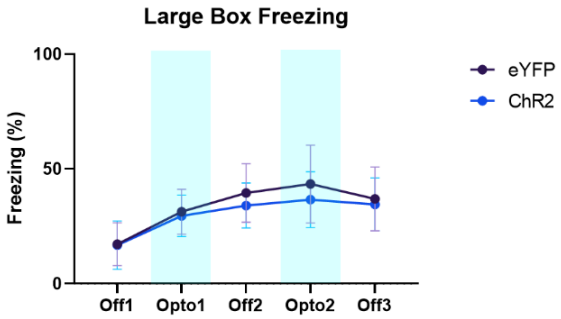

Figure 26. Freezing behavior (%) of control animals and animals who experienced optogenetic activation of a fear memory in a large box.

The freezing behavior of the animals in the PAG fiber photometry experiment group during optogenetic activation in a large box can be seen in Figure 26. There was no effect of optogenetic fear engram activation or of treatment on freezing behavior in a small environment (RM 2-way ANOVA; interaction: F (4, 32) = 0.05935, P=0.9931, Time: F (2.245, 17.96) = 2.759, P=0.0852, Treatment: F (1, 8) = 0.06150, P=0.8104).

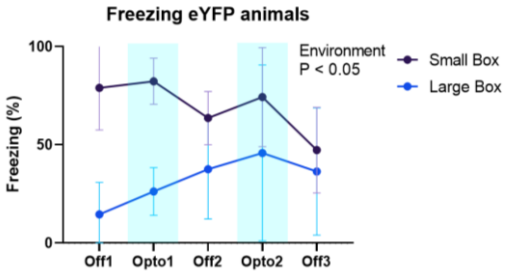

Figure 27. Freezing behavior (%) of eYFP animals in a small and large box.

The freezing behavior of the eYFP animals in the PAG fiber photometry experiment group during optogenetic activation in a small and large box can be seen in Figure 27. It was found that there was a significant effect of environment size on freezing percentage where eYFP animals spent significantly more time freezing in the small box than in the large box. However, no effect of optogenetic activation was found on freezing. (RM 2-way ANOVA; interaction: F (4, 24) = 1.546, P=0.2208, Time: F (2.088, 12.53) = 0.4932, P=0.6297, environment: F (1, 6) = 6.500, P=0.0435).

The freezing behavior of the ChR2 animals in the PAG fiber photometry experiment group during optogenetic activation in a small and large box can be seen in Figure 28. It was found that there was no significant effect of both environment size and optogenetic activation on freezing (RM 2-way ANOVA; interaction: F (4, 40) = 0.4501, P=0.7717, Time: F (1.971, 19.71) = 0.8921, P=0.4243, environment: F (1, 10) = 3.737, P=0.0820).

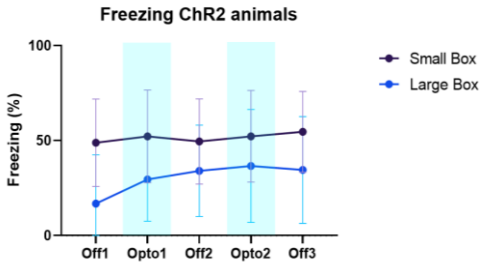

Figure 28. Freezing behavior (%) of eYFP animals in a small and large box.

Overall, both eYFP and ChR2 animals show similar amounts of freezing during CFC and in the small and large environments across epochs when comparing the two groups. However, when comparing the two groups separately in the two differently sized environments, an effect is found as eYFP animals freeze significantly more in a small environment while there is a trend for this effect for ChR2 animals. Surprisingly, all animals do not show any light-induced freezing in small and large environments.

3.4 PAG neuronal activity

To further dive deeper into the neuronal processes occurring in the brain, during light-induced freezing in different contexts, neuronal activity was measured in the PAG. We hypothesized that there would be more neuronal activity in the PAG during freezing and, as we hypothesized that animals would freeze more in the small environment, we hypothesized that there would be more neuronal activity in the PAG in the small environment than in the large environment.

Representative neuronal activity of animals during CFC and optogenetic activation in a small and large box can be seen in Figure 29 together with multiple peri-event analyses. In Figure 29A an example of an animal with good signal is shown in the CFC paradigm. Four peaks in the GCaMP signal can be seen in this figure, immediately following the delivery of foot shocks at 200, 280, 360, and 440 seconds. The representative neuronal activity of the same animal during the optogenetic activation trials can be seen in Figure 29B-C. To test whether PAG neurons respond specifically to footshock, a peri-event analysis was performed to determine if calcium transients were temporally locked to the footshock. This result can be seen in Figure 29D and although no statistical analysis has been performed on this result, it is visible that the df/F increased for both the ChR2 and eYFP animals after the onset of each footshock. Additionally, a peri-event analysis was performed to determine if calcium transients were temporally locked to the freezing onset of offset of animals during CFC

(Figure 29 E, F). Again, no statistical analysis was performed on this data, but there does seem to be a slight increase in df/F before onset of freezing behavior during CFC. There does not seem to be a specific increase or decrease in df/F around the offset of freezing behavior during CFC. For the animals in the small and large box, a peri-event test was performed to determine if calcium transients were temporally locked to the onset of optogenetic light stimulation in both the small and large box (Figure 29G, H). Although no statistical test has been performed on this data, the onset of optogenetic light stimulation seems to be followed by an increase of df/F for ChR2 animals in the large box, while the eYFP animals do not show this increase. In the small box, no clear change of df/F can be seen for both groups at the onset of optogenetic light stimulation. Another peri-event test was performed to determine if calcium transients were temporally locked to the onset and offset of freezing behavior for the small and large box (Figure 29I-L). There does not seem to be a change in df/F at the onset and offset of freezing behavior between the eYFP and ChR2 animals in both environments.

Additionally, specific event metrics were calculated such as peak height, full-width half max (FWHM), area under the curve (AUC), and event frequency (events/minute) for the animals during CFC and in both the small and large environment (Figure 30). The results showed that there was no significant difference in peak height between eYFP and ChR2 animals during CFC (two-tailed Mann Whitney test; $U = 1.5$, $P = 0.4000$), in the small box (two-tailed Mann Whitney test; $U = 2$, $P=0.5333$) and in the large box (two-tailed Mann Whitney test; $U = 3$, $P = 0.8000$) (Figure 30 A, E, I). The results further showed that there was no significant difference in FWHM between eYFP and ChR2 animals during CFC (two-tailed Mann Whitney test; $U = 0$, $P = 0.1333$), in the small box (two-tailed Mann Whitney test; $U = 0$, $P = 0.1333$) and in the large box (two-tailed Mann Whitney test; $U = 3$, $P = 0.8000$) (Figure 30 B, F, J). Furthermore, the results showed that there was no significant difference in the area under the curve between eYFP and ChR2 animals during CFC (two-tailed Mann Whitney test; $U = 1$, $P = 0.2667$), in the small box (two-tailed Mann Whitney test; $U = 4$, $P >0.9999$) and in the large box (two-tailed Mann Whitney test; $U = 4$, $P >0.9999$) (Figure 30 C, G, K,). Lastly, the results showed that there was no difference in event frequency between the eYFP and ChR2 animals during CFC (two-tailed Mann Whitney test; $U = 0$, $P = 0.1333$), in the small box (two-tailed Mann Whitney test; $U = 3$, $P = 0.9333$) and in the large box (two-tailed Mann Whitney test; $U = 3$, $P = 0.9333$) (Figure 30 D, H, L).

Overall, it is shown that there is a clear increase in neuronal activity in the PAG following the experience of a foot shock. Furthermore, it also seems like there is an increase in PAG neuronal activity following the onset of optogenetic light stimulation in the large box for ChR2 animals. Other than that, no significant differences can be found when comparing different event metrics of animals over the different light epochs in a small and large environment.

Figure 29. PAG neuronal activity. (A) Representative calcium time series (dF/F %) for shock and no-shock conditions during the 360 second CFC session. 1.5mA foot shocks occurred at the 120, 180, 240 and 300 second time points, as indicated by vertical dashed lines. (B) Representative calcium time series (dF/F %) during optogenetic stimulation in a small box. (C) Representative calcium time series (dF/F %) during optogenetic stimulation in a large box. (D) Peri-event analysis for 1.5 mA foot shock, with the onset of foot shock occurring at the dashed line (time = 0). (E) Peri-event analysis for the start of freezing behavior during fear conditioning (time = 0). (F) Peri-event analysis for the end of freezing behavior during fear conditioning (time = 0). (G) Peri-event analysis for the start of optogenetic light stimulation in the large box (time = 0). (H) Peri-event analysis for the start of optogenetic light stimulation in the small box (time = 0). (I) Peri-event analysis for the start of freezing behavior in the small box (time = 0). (J) Peri-event analysis for the end of freezing in the small box (time = 0). (K) Peri-event analysis for the start of freezing behavior in the large box (time = 0). (L) Peri-event analysis for the end of freezing behavior in the large box (time = 0).

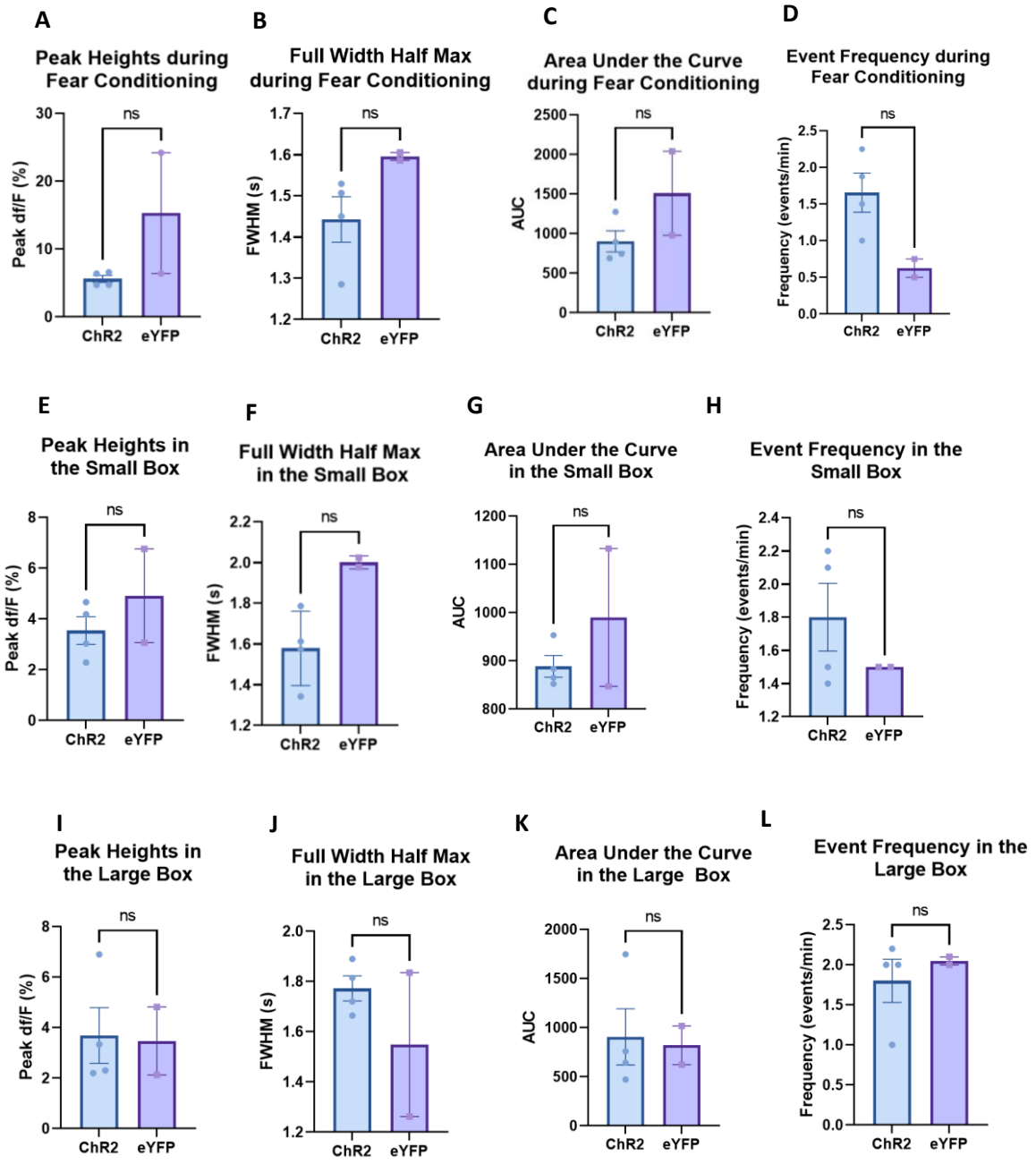

Figure 30. Calcium event metrics. (A) Peak heights during fear condition. (B) Full width half max during fear conditioning. (C) Area under the curve during fear conditioning. (D) Event frequency during fear conditioning. (E) Peak heights in the small box. (F) Full width half max in the small box. (G) Area under the curve in the small box. (H) Event frequency in the small box. (I) Peak heights in the large box. (J) Full width half max in the large box. (K) Area under the curve in the large box. (L) Event frequency in the large box.

4. Discussion

To investigate the effect of optogenetic activation of a fear memory on fear behavior and the involvement of different brain regions in this behavior, we perturbed and observed different downstream areas of the HC. We inhibited the LHA and analyzed freezing behavior and $cFos^+$ cell counts. Additionally, we investigated PAG neuronal activity together with freezing behavior while experimental animals experienced optogenetic activation of fear memory engrams. The results from these experiments will be discussed below.

4.1 Chemogenetic LHA silencing diminishes freezing behavior

To test the effect of DREADD silencing of the LHA on fear behavior, we examined the freezing behavior of both DREADD and control animals. Because literature shows that the LHA is involved in freezing behavior, we hypothesized that inhibiting the LHA would decrease freezing. The results showed that animals that underwent chemogenetic LHA inhibition exhibited near floor-levels of freezing. This indicates that proper LHA functioning is crucial for the display of freezing behavior.

This finding is in line with previous research of Soya et al. (2013) who shows that mice that do not express the Hcrt-1 receptor, a distinct cell population uniquely residing within the LHA, show impaired freezing responses in fear-conditioning paradigms. On the other side, Tully (2015) also looks at the effect of DREADD silencing of the LHA on freezing and observes that LHA silencing does not alter learned fear response in a contextual fear memory expression. They suggest that the medial hypothalamic area is important for cued fear conditioning, while the LHA is in innate threat response. Although, when observing brain images, it did not seem like there was a lot of virus spread to the medial hypothalamic area, it could be possible some of this area got inhibited as well. However, the difference in freezing behavior between the control and DREADD group was so large that it does not seem likely that the small amounts of DREADD virus spreading into the medial hypothalamus could be responsible for this big effect.

4.2 CNO injected animals do not display light-induced freezing

Furthermore, we examined the freezing behavior of both DREADD and control animals across different light epochs. While we hypothesized that DREADD animals would show reduced freezing, it was also predicted that control animals would show the light-induced freezing response observed in previous studies. However, surprisingly, the results show that control animals do not show light-induced freezing.

One explanation for this finding is that CNO could have off-target effects. Although the control animals were injected with an empty virus and therefore should not have been affected by the DREADDS, they did receive a CNO injection, which could have influenced their behavior. The use of DREADDS is a popular tool in neuroscience to manipulate neuronal activity. This functionality is based on the assumption that CNO itself does not have any *in vivo* effects at non-DREADD targets. However, recent studies have called this notion into question as it has been recently reported that CNO can reverse-metabolize to its parent compound clozapine which can have several physiological and behavioral effects. One study shows that the administration of 1.0–20.0 mg/kg of CNO in Long-Evans rats decreased D-amphetamine-induced hyperlocomotion (MacLaren et al., 2016). Another study finds that a clozapine dose of 0.05-1 mg/kg reduces locomotion, increases anxiety, and increases cognitive flexibility (Ilg et al., 2018). The same increase in anxiety is also found by Pomrenze et al. (2019) with low doses of CNO injections. Both the increased anxiety and the reduced locomotion could be responsible for the observed freezing behavior in control animals. First of all, the increased anxiety levels may have already brought the mice to a state of heightened fear, which caused the light-induced activation of a fear memory to be less impactful in terms of inducing further fear responses and subsequent freezing behavior. In other words, the mice may have already reached a maximum level of fear due to increased anxiety, making them less responsive to additional fear-inducing stimuli. Secondly, the reduced locomotion that clozapine is responsible for could also have contributed to the

increased levels of freezing that were measured because of decreased overall motion. In future research, these off-target effects could be prevented by adding a second control group that would receive the same treatment as the CNO control group, but instead of CNO, they would be injected with saline. This would allow us to determine whether CNO has off-target effects that influences recorded freezing behavior. An alternative approach to prevent the effect of reverse-metabolization of CNO is using another DREADD ligand that cannot be transformed into a clozapine-like compound 21 (Chen et al., 2015).

Another explanation for this finding is generalization. Sometimes, mice are unable to distinguish two contexts and will show freezing behavior in the context that is supposed to be neutral. The mice might have associated the neutral context with the CFC context because they are similar in size and appearance. Because of this, the animals could have responded to the memory of CFC in the absence of light-induced activation of this memory and started freezing. This could have rendered the effect of light-induced activation of the fear memory useless. In future studies, an odor could be used to help eliminate the effect of generalization as it is found by Huckleberry et al. (2016) that odor is a very salient feature.

4.3 Chemogenetically inhibiting the LHA increases cFos expression

To gain histological insight, we measured endogenous cFos expression in the LHA by the number of $cFos^+$ cells after optogenetic fear memory activation. We hypothesized that, because we were inhibiting the LHA, there would be less activity in this area and therefore also lower cFos expression and therefore fewer $cFos^+$ cells. Surprisingly, the results show that animals who experienced chemogenetic LHA silencing had a significantly higher amount $cFos^+$ cells than control animals. This was unexpected as it was hypothesized that chemogenetic silencing would decrease activity and therefore decrease the amount of cFos+ cells.

One explanation for this finding is that neighboring neurons might have compensated for the inhibition and started increasing their activity which caused increased cFos expression in the local area. It has been suggested that neural networks prefer to be in a balanced state of excitatory and inhibitory activity. For example, acute experimental manipulations that selectively decrease either inhibition or excitation cause a shift in cortical activity to a hyperexcitable or silent state (Dudek & Sutula, 2007). Furthermore, excitation and inhibition respectively increase and decrease together during physiological cortical activity in a study by Van Vreeswijk & Sompolinsky (1996). This could suggest that the sudden inhibition of a part of the neurons in the LHA could have caused stark excitation in other neurons in the LHA, which created this increase in cFos expression. This could be examined in future research by investigating the overlap between $cFos^+$ cells and DREADD cells. If these do not overlap, it is an indication that the increased cFos expression is due to a compensation mechanism.

Another explanation for this finding is that the increased cFos expression is not a result of the chemogenetic inhibition, but a result of the termination of chemogenetic inhibition causing a resurgence of neuronal activity which lead to a spike in cFos expression. A study by Jendryka et al. (2019) shows that at 60 minutes after an intraperitoneal CNO injection, no CNO can be detected in the cortex (Jendryka et al., 2019). As CNO needs to be present for chemogenetic inhibition, at this time point, LHA neurons could be resuming activity. The animals were perfused at 120 minutes past CNO injection which means that at that time point, there were 60 minutes left before the brains were extracted and fixed. According to a study by Zhong et al. (2014), 60 minutes is sufficient for measuring increased cFos expression following an experience. Therefore, the increased cFos expression may not have been a result of the chemogenetic inhibition, but from the end of inhibition and the reactivation of neurons, which resulted in increased cFos expression.

Another point to note for this result is that cFos not only is a marker of neuronal activity but is also believed to be an important mediator of activity-dependent neuroplasticity (Sheng & Greenberg, 1990). In the HC, for example, cFos expression is highly correlated with environment novelty but not

complexity (VanElzakker et al., 2008). Furthermore, it is found that cFos has a causal role in shaping the place codes by encoding accurate, stable, and spatially uniform maps (Pattit et al., 2022). Another study has noted that it is too short-sighted to see cFos simply as a marker of neuronal activity as cFos mRNA expression because of kindled seizures does not reliably increase with neuronal firing (Labiner et al., 1993). Although no studies could be found on the different roles of cFos in the LHA, these studies show that increased cFos levels do not necessarily indicate increased neuronal firing, but can also represent other processes that are happening in the brain area. More research about the differential influences of cFos in this brain area will be needed to conclude more about what increased cFos expression signals.

4.4 ChR2 animals showed no effect of light-induced fear memory activation on freezing behavior in the PAG photometry experiment

We wanted to test if the light-induced freezing would be different in a small or a large environment. The hypothesis was that ChR2 animals would show light-induced freezing in both the small and large environments, but that there would be more light-induced freezing in the small environment than the large environment. However, we did not find light-induced freezing in the small or large environment for the ChR2 animals.

A possible explanation for this non-effect could be that the animals were experiencing extremely high levels of anxiety. This could have diminished the impact of the optogenetically activated fear memory leading to similar freezing levels between the light-on and light-off periods. That the animals experienced high levels of anxiety can be concluded from the percentages that they spent freezing. In the small box, the ChR2 animals had a mean freezing percentage of 51.50% while the eYFP group had an even higher mean of 60.86%. During CFC, this amount of freezing was only reached after having experienced 3 shocks. This suggests that the animals in the small box were already experiencing high anxiety levels without optogenetic fear memory activation. Because of this, the effect of optogenetic stimulation on freezing behavior could be negligible. There could be several explanations for these high levels of anxiety.

One explanation is that the animals were generalizing the CFC chamber to the small box. Because we used the same sized box for the small environment as for the CFC chamber it could be possible that the animals were confusing this environment with the CFC one. This generalization could have caused their high levels of anxiety. Although we used wall and floor inserts and different odors to allow for discrimination between the CFC chamber, in future research, CFC could be done in a medium-sized box. This would help reduce the anxiety caused by generalization.

Another possibility is that the animals were experiencing this high level of fear because plugging in the two optogenetic fibers and the fiber photometry fiber was not always a smooth process. Because we were still getting used to the motions of plugging in the animals, our stress and struggles with this procedure might have contributed to the animals' heightened stress levels. For future research, it might be beneficial to habituate the animals to the plugging in and plugging out of the fibers. Then, the animals might be less scared and show a more pronounced effect of optogenetic fear memory activation.

4.5 Environmental size only influenced freezing in eYFP, not ChR2 animals

To test for an effect of environmental size on freezing, we examined freezing percentages of both ChrR2 and eYFP animals between the small and large environments across light epochs. It was first hypothesized that only ChR2 animals would show significant amounts of freezing, however when observing the high freezing amounts of both groups of animals, we also examined if there was an effect of environmental size on freezing behavior of both eYFP and ChR2 animals. The results from the PAG experimental group demonstrated that eYFP, not ChR2, animals freeze more in the small environment than animals in the large environment.

The finding that animals show more freezing behavior in a smaller environment is also found by Rosen et al. (2008). This increased freezing in a small environment is explained by the inability to avoid the source of fear. For the animals in this experiment, this explanation is not directly applicable, as there is no direct source that elicits the fear. It is possible that the animals sensed a higher chance of escaping from a possible threat in the large environment, leading to reduced freezing behavior. If this is the case, it could be possible that the animals expressed more locomotion behavior as they would have been searching for an escape. This could be a possible factor to include and investigate in future research.

Another possible explanation for this finding is that the control animals were generalizing. As previously mentioned, the small box was a similar size to the CFC chamber which could have led to generalization. In future research, to prevent this, CFC could be done in a medium-sized box that is used for rats. Additionally, a limitation of this study is the fact that there was no counterbalancing for the order that the animals are tested in the environments. For future research, it is suggested to include counterbalancing.

However, as this difference in freezing is significant for eYFP animals, no significant difference in environmental size on freezing was found in ChR2 animals during the light-on and light-off epochs. A trend, however, could be found for this effect in this group as the p is 0.0820. Future studies can repeat this experiment and add more experimental animals to clarify whether there actually is a difference in freezing levels between the two environments for the experimental animals.

4.5 PAG neuronal activity increased at shock onset during CFC

Because we wanted to get a better understanding of what happens in the brain during light-induced freezing in different environmental sizes, PAG neuronal activity was measured. We hypothesized that animals would show more PAG neuronal activity during freezing behavior and they would therefore also show increased activity during light-on epochs, after the onset of freezing behavior, and after or during the delivery of a footshock.

Although there appeared to be an increase in PAG neuronal activity preceding the onset of freezing behavior during CFC and following the onset of optogenetic light stimulation in the large box, the lack of statistical analysis on this data limits definitive conclusions. For future research, it is recommended to increase the sample size and to perform thorough statistical analyses. However, the results did demonstrate a clear increase in PAG neuronal activity following the experience of a foot shock during CFC. Although this data was also not statistically analyzed, the effect was prominent and warrants further discussion, while acknowledging the speculative nature of any conclusions drawn. While the PAG is a common output area for defensive behavior, the PAG is also involved in integrating nociceptive inputs from the spinal and trigeminal horn to the BLA (Johansen et al., 2010). This suggests that the observed increase in PAG activity could be attributed to either the perception of the painful stimulus itself or the defensive response elicited by the stimulus. The PAG neuronal activity data regarding the on- and offset of freezing behavior can clarify this. This data suggests that PAG neuronal activity increases right before the onset of freezing behavior for animals in the CFC group. However, this pattern is not as apparent in animals in the small or large environments. For the neuronal activity at the offset of freezing behavior, no clear trend can be seen. Since no statistical analysis was conducted on this data, no definitive conclusions can be drawn from these findings. However, future research could investigate whether the PAG is more prominently involved in freezing behavior triggered by sensory stimuli or memory-driven responses. Performing a rigorous statistical analysis would provide further insights into the specific roles of the PAG in different contexts of freezing behavior.

4.6 Similar measures of peak height, full-width half max, area under the curve, and frequency between eYFP and ChR2 animals

Additionally, we calculated specific event metrics such as peak height, full-width half max, area under the curve, and frequency during CFC and in both the small and large environment. We hypothesized that these metrics would be higher in ChR2 animals than in eYFP animals. The results showed that none of the event metrics were significantly different between ChR2 and eYFP animals for any of the conditions. This suggests that there is no difference in neuronal signal in the PAG between control and experimental animals, indicating that optogenetic activation of a fear memory does not influence PAG neuronal activity.

This result is not completely surprising as the freezing behavior also did not differ between the control and experimental animals. If the amount of freezing behavior is correlated with PAG neuronal activity, the absence of a difference in freezing between the groups suggests that there should also be no difference in PAG neuronal activity between the groups. As mentioned before, this could be attributed to the stress experienced during the process of acclimating to plugging in animals and generalisation. This could be prevented in future research by habituating the animals to the plugging in of the fibers and fear conditioning in a medium-sized chamber. Another reason why there were no significant differences between the groups is that the number of animals used in this analysis is extremely low. To be able to have more clear results and to be able to draw any conclusions out of this data, more animals have to be added to the analysis.

4.7 Implications and future studies

For future research, multiple proposals have been already made to improve the research that has been described in this thesis. Based on the findings of this thesis, there are multiple possibilities for future research to further examine the role of engrams in the brain and behavior. Firstly, exploring the role of other brain regions, such as the amygdala, in fear behavior and investigating their neuronal activity in various environmental sizes could provide valuable insights into the complex network of brain regions underlying fear processing. Based on the importance of the amygdala in fear behavior, we expect that amygdala activity would be higher during optogenetic stimulation of a fear memory in a small environment. Another suggestion for future research would be to investigate flight behavior and PAG neuronal activity during the display of this behavior. According to the threat-imminence model, fight or flight behavior would be shown after freezing behavior when emotional intensity or imminence is increased. As the PAG is also involved in this behavior we would expect that the occurrence of this behavior would be paired with increased PAG activity. Additionally, as it has been suggested that the LHA is also involved in innate fear, it would be interesting to see the effect of chemogenetic inhibition on freezing behavior during the exposure to, for example, a looming shadow or a natural predator. We would expect that freezing levels would also be diminished in this experiment. Lastly, incorporating other environmental factors, such as hiding places, into a study such as this would further explore the influence of the environment during optogenetic fear memory activation on defensive behavior.

The findings of this study have several implications for our knowledge of the fear network and its role in neuropsychiatric disorders. The research on the effect of engrams on the brain and behavior will give more insight into which brain areas contribute to negative emotions, fear, and psychiatric disorders and how this is organized. This knowledge can help further the development of therapeutic interventions aimed at alleviating the symptoms of these disorders and improving the lives of those affected. By gaining more knowledge of the fear memory network, we can better target the underlying causes of negative affective states and potentially reduce the negative consequences of these disorders in society.

4.8 Conclusions

Based on the results, we conclude that LHA activity is necessary for freezing behavior. Furthermore, we conclude that a CNO injection diminishes light-induced freezing, possibly by causing off-target anxiogenic effects. Additionally, we conclude that animals freeze more in a small environment than in a large environment. Lastly, we conclude that the reception of a foot shock increases PAG neuronal activity.

These findings are significant to the research of psychiatric disorders as they help understand the neuronal circuits behind the dysregulation of fear and anxiety. By revealing the role of the LHA in freezing behavior and the influence of environmental factors, as well as the involvement of PAG signaling, this work could help in the development of targeted interventions and therapies for psychiatric disorders characterized by abnormal fear and anxiety responses.

5. References

Aggleton, J. P., & Brown, M. W. (1999). Episodic memory, amnesia, and the hippocampal–anterior thalamic axis. *Behavioral and brain sciences*, 22(3), 425-444.

Alexander, G. M., Rogan, S. C., Abbas, A. I., Armbruster, B. N., Pei, Y., Allen, J. A., ... & Roth, B. L. (2009). Remote control of neuronal activity in transgenic mice expressing evolved G protein-coupled receptors. *Neuron*, 63(1), 27-39.

Armbruster, B. N., Li, X., Pausch, M. H., Herlitze, S., & Roth, B. L. (2007). Evolving the lock to fit the key to create a family of G protein-coupled receptors potently activated by an inert ligand. *Proceedings of the National Academy of Sciences*, 104(12), 5163-5168.

Asok, A., Kandel, E. R., & Rayman, J. B. (2019). The neurobiology of fear generalization. *Frontiers in behavioral neuroscience*, 12, 329.

Bailey, C. H., Bartsch, D., & Kandel, E. R. (1996). Toward a molecular definition of long-term memory storage. *Proceedings of the National Academy of Sciences*, 93(24), 13445-13452.

Baldi, E., Lorenzini, C. A., & Bucherelli, C. (2004). Footshock intensity and generalization in contextual and auditory-cued fear conditioning in the rat. *Neurobiology of learning and memory*, 81(3), 162-166.

Beckers, T., Krypotos, A. M., Boddez, Y., Effting, M., & Kindt, M. (2013). What's wrong with fear conditioning?. *Biological psychology*, 92(1), 90-96.

Belova, M. A., Paton, J. J., Morrison, S. E., & Salzman, C. D. (2007). Expectation modulates neural responses to pleasant and aversive stimuli in primate amygdala. *Neuron*, 55(6), 970-984.

Benarroch, E. E. (2012). Periaqueductal gray: an interface for behavioral control. *Neurology*, 78(3), 210-217.

Bernardis, L. L., & Bellinger, L. L. (1993). The lateral hypothalamic area revisited: neuroanatomy, body weight regulation, neuroendocrinology and metabolism. *Neuroscience & biobehavioral reviews*, 17(2), 141-193.

Berthoud, H. R., & Münzberg, H. (2011). The lateral hypothalamus as integrator of metabolic and environmental needs: from electrical self-stimulation to opto-genetics. *Physiology & behavior*, 104(1), 29-39.

Blanchard, D. C., & Blanchard, R. J. (2008). Chapter 2.4 Defensive behaviors, fear, and anxiety. In *Handbook of Behavioral Neuroscience* (pp. 63–79). Elsevier BV. https://doi.org/10.1016/s1569-7339(07)00005-7

Blanchard, D. C., Griebel, G., & Blanchard, R. J. (2001). Mouse defensive behaviors: pharmacological and behavioral assays for anxiety and panic. *Neuroscience & Biobehavioral Reviews*, 25(3), 205-218.

Blanchard, D. C., Griebel, G., Pobbe, R. L., & Blanchard, R. J. (2011). Risk assessment as an evolved threat detection and analysis process. *Neuroscience & Biobehavioral Reviews*, 35(4), 991–998. https://doi.org/10.1016/j.neubiorev.2010.10.016

Blanchard, D. C., Hynd, A. L., Minke, K. A., Minemoto, T., & Blanchard, R. J. (2001). Human defensive behaviors to threat scenarios show parallels to fear-and anxiety-related defense patterns of non-human mammals. *Neuroscience & Biobehavioral Reviews*, 25(7-8), 761-770.

Blanchard, R. J. (2008). Handbook of Anxiety and Fear. In *Handbook of Behavioral Neuroscience*. Elsevier BV. https://doi.org/10.1016/s1569-7339(07)x0001-8

Blanchard, R. J., & Blanchard, D. C. (1969). Crouching as an index of fear. *Journal of comparative and physiological psychology*, 67(3), 370.

Blanchard, R. J., & Blanchard, D. C. (1989). Antipredator defensive behaviors in a visible burrow system. *Journal of comparative psychology*, 103(1), 70.

Boer, A. R. D. (2021). Behavioral and neurobiological correlates of dominance ranking in mixed-sex colonies of wild-type rats (Doctoral dissertation).

Bolles, R. C. (1970). Species-specific defense reactions and avoidance learning. *Psychological review*, 77(1), 32.

Bolles, R. C., & Collier, A. C. (1976). The effect of predictive cues on freezing in rats. *Animal Learning & Behavior*, 4(1), 6-8.

Bonnavion, P., Jackson, A. C., Carter, M. E., & De Lecea, L. (2015). Antagonistic interplay between hypocretin and leptin in the lateral hypothalamus regulates stress responses. *Nature communications*, 6(1), 1-14.

Bonnavion, P., Mickelsen, L. E., Fujita, A., De Lecea, L., & Jackson, A. C. (2016). Hubs and spokes of the lateral hypothalamus: cell types, circuits and behaviour. *The Journal of physiology*, 594(22), 6443-6462.

Bordi, F., & LeDoux, J. E. (1994). Response properties of single units in areas of rat auditory thalamus that project to the amygdala: II. Cells receiving convergent auditory and somatosensory inputs and cells antidromically activated by amygdala stimulation. *Experimental Brain Research*, 98, 275-286.

Boyden, E. S., Zhang, F., Bamberg, E., Nagel, G., & Deisseroth, K. (2005). Millisecond-timescale, genetically targeted optical control of neural activity. *Nature neuroscience*, 8(9), 1263-1268.

Brandão, M. L., Zanoveli, J. M., Ruiz-Martinez, R. C., Oliveira, L. C., & Landeira-Fernandez, J. (2008). Different patterns of freezing behavior organized in the periaqueductal gray of rats: association with different types of anxiety. *Behavioural brain research*, 188(1), 1-13.

Brown, J. A., Woodworth, H. L., & Leinninger, G. M. (2015). To ingest or rest? Specialized roles of lateral hypothalamic area neurons in coordinating energy balance. *Frontiers in systems neuroscience*, 9, 9.

Burdakov, D., Karnani, M. M., & Gonzalez, A. (2013). Lateral hypothalamus as a sensor-regulator in respiratory and metabolic control. *Physiology & behavior*, 121, 117-124.
Campbell, E. J., & Marchant, N. J. (2018). The use of chemogenetics in behavioural neuroscience: receptor variants, targeting approaches and caveats. *British journal of pharmacology*, 175(7), 994-1003.
Chen, T. W., Wardill, T. J., Sun, Y., Pulver, S. R., Renninger, S. L., Baohan, A., ... & Kim, D. S. (2013). Ultrasensitive fluorescent proteins for imaging neuronal activity. *Nature*, 499(7458), 295-300.
Chen, X., Choo, H., Huang, X. P., Yang, X., Stone, O., Roth, B. L., & Jin, J. (2015). The first structure–activity relationship studies for designer receptors exclusively activated by designer drugs. *ACS chemical neuroscience*, 6(3), 476-484.
Cheriyan, J., & Sheets, P. L. (2018). Altered excitability and local connectivity of mPFC-PAG neurons in a mouse model of neuropathic pain. *Journal of Neuroscience*, 38(20), 4829-4839.
Clark, R. E., Broadbent, N. J., & Squire, L. R. (2005). Impaired remote spatial memory after hippocampal lesions despite extensive training beginning early in life. *Hippocampus*, 15(3), 340-346.
Clarke, R. W., & Harris, J. (2004). The organization of motor responses to noxious stimuli. *Brain research reviews*, 46(2), 163-172.
Curzon, P., Rustay, N. R., & Browman, K. E. (2008). Cued and Contextual Fear Conditioning for Rodents. In *Frontiers in neuroscience* (pp. 19–37). CRC Press. https://doi.org/10.1201/noe1420052343.ch2
D, C. P., & Schacter, D. L. (1983). Stranger behind the Engram: Theories of Memory and the Psychology of Science. *American Journal of Psychology*, *96*(3), 427. https://doi.org/10.2307/1422334
Deisseroth, K. (2011). Optogenetics. *Nature methods*, 8(1), 26-29.
Deisseroth, K. (2015). Optogenetics: 10 years of microbial opsins in neuroscience. *Nature neuroscience*, 18(9), 1213-1225.
Deng, H., Xiao, X., & Wang, Z. (2016). Periaqueductal gray neuronal activities underlie different aspects of defensive behaviors. *Journal of Neuroscience*, 36(29), 7580-7588.
Diekelmann, S., & Born, J. (2010). The memory function of sleep. Nature *Reviews Neuroscience*, 11(2), 114-126.
Dudek, F. E., & Sutula, T. P. (2007). Epileptogenesis in the dentate gyrus: a critical perspective. *Progress in brain research*, 163, 755-773.
Eichenbaum, H. (2000). A cortical–hippocampal system for declarative memory. *Nature reviews neuroscience*, 1(1), 41-50.
Elliott, N. D., & Richardson, R. (2019). The effects of early life stress on context fear generalization in adult rats. *Behavioral Neuroscience*, 133(1), 50.
Elzinga, B. M., & Bremner, J. D. (2002). Are the neural substrates of memory the final common pathway in posttraumatic stress disorder (PTSD)?. *Journal of affective disorders*, 70(1), 1-17.
Fadok, J. P., Krabbe, S., Markovic, M., Courtin, J., Xu, C., Massi, L., ... & Lüthi, A. (2017). A competitive inhibitory circuit for selection of active and passive fear responses. *Nature*, 542(7639), 96-100.
Fanselow, M. S. (1989). The Adaptive Function of Conditioned Defensive Behavior: An Ecological Approach to Pavlovian Stimulus-Substitution Theory. In *Springer eBooks* (pp. 151–166). https://doi.org/10.1007/978-94-009-2403-1_9
Fanselow, M. S. (1991). The Midbrain Periaqueductal Gray as a Coordinator of Action in Response to Fear and Anxiety. *In Springer eBooks* (pp. 151–173). https://doi.org/10.1007/978-1-4615-3302-3_10
Fanselow, M. S. (1994). Neural organization of the defensive behavior system responsible for fear. *Psychonomic bulletin & review*, 1(4), 429-438.
Fanselow, M. S., & Dong, H. W. (2010). Are the dorsal and ventral HC functionally distinct structures?. *Neuron*, 65(1), 7-19.
Fanselow, M. S., & Lester, L. S. (2013). A Functional Behavioristic Approach to Aversively Motivated Behavior:: Predatory Imminence as a Determinant of the Topography of Defensive Behavior. In *Evolution and learning* (pp. 185-212). Psychology Press.
Felix-Ortiz, A. C., Beyeler, A., Seo, C., Leppla, C. A., Wildes, C. P., & Tye, K. M. (2013). BLA to vHPC inputs modulate anxiety-related behaviors. *Neuron*, 79(4), 658-664.
Geeraedts, L. M. G., Nieuwenhuys, R., & Veening, J. G. (1990). Medial forebrain bundle of the rat: IV. Cytoarchitecture of the caudal (lateral hypothalamic) part of the medial forebrain bundle bed nucleus. *Journal of Comparative Neurology*, 294(4), 537-568.
Gerber, B., Tanimoto, H., & Heisenberg, M. (2004). An engram found? Evaluating the evidence from fruit flies. *Current opinion in neurobiology*, 14(6), 737-744.
Giardino, W. J., & de Lecea, L. (2014). Hypocretin (orexin) neuromodulation of stress and reward pathways. *Current opinion in neurobiology*, 29, 103-108.
González, J. A., Iordanidou, P., Strom, M., Adamantidis, A., & Burdakov, D. (2016). Awake dynamics and brain-wide direct inputs of hypothalamic MCH and orexin networks. *Nature communications*, 7(1), 1-9.

Graziano, M. S., & Cooke, D. F. (2006). Parieto-frontal interactions, personal space, and defensive behavior. *Neuropsychologia*, 44(6), 845-859.
Grillon, C., & Baas, J. (2003). A review of the modulation of the startle reflex by affective states and its application in psychiatry. *Clinical neurophysiology*, 114(9), 1557-1579.
Gunaydin, L. A., Grosenick, L., Finkelstein, J. C., Kauvar, I. V., Fenno, L. E., Adhikari, A., ... & Deisseroth, K. (2014). Natural neural projection dynamics underlying social behavior. *Cell*, 157(7), 1535-1551.
Guo, Q., Zhou, J., Feng, Q., Lin, R., Gong, H., Luo, Q., ... & Fu, L. (2015). Multi-channel fiber photometry for population neuronal activity recording. *Biomedical optics express*, 6(10), 3919-3931.
Hahn, J. D., & Swanson, L. W. (2010). Distinct patterns of neuronal inputs and outputs of the juxtaparaventricular and suprafornical regions of the lateral hypothalamic area in the male rat. *Brain research reviews*, 64(1), 14-103.
Hahn, J. D., & Swanson, L. W. (2015). Connections of the juxtaventromedial region of the lateral hypothalamic area in the male rat. *Frontiers in systems neuroscience*, 9, 66.
Hansson, L. (2002). Quality of life in depression and anxiety. *International Review of Psychiatry*, 14(3), 185-189.
Haubensak, W., Kunwar, P. S., Cai, H., Ciocchi, S., Wall, N. R., Ponnusamy, R., ... & Anderson, D. J. (2010). Genetic dissection of an amygdala microcircuit that gates conditioned fear. *Nature*, 468(7321), 270-276.
Helmstetter, F. J., & Fanselow, M. S. (1993). Aversively motivated changes in meal patterns of rats in a closed economy: The effects of shock density. *Animal Learning & Behavior*, 21(2), 168-175.
Hinrichs, W., Kisker, C., Düvel, M., Müller, A., Tovar, K., Hillen, W., & Saenger, W. (1994). Structure of the Tet repressor-tetracycline complex and regulation of antibiotic resistance. *Science*, 264(5157), 418-420.
Hinton, D. E., Lewis-Fernández, R., & Pollack, M. H. (2009). A model of the generation of ataque de nervios: The role of fear of negative affect and fear of arousal symptoms. *CNS neuroscience & therapeutics*, 15(3), 264-275.
Huckleberry, K. A., Ferguson, L. B., & Drew, M. R. (2016). Behavioral mechanisms of context fear generalization in mice. *Learning & memory*, 23(12), 703-709.
Hunsperger, R. W. (1963). Comportements affectifs provoqués par la stimulation électrique du tronc cérébral et du cerveau antérieur (Doctoral dissertation, Verlag nicht ermittelbar).
Hurley, S. W., & Johnson, A. K. (2014). The role of the lateral hypothalamus and orexin in ingestive behavior: a model for the translation of past experience and sensed deficits into motivated behaviors. *Frontiers in systems neuroscience*, 8, 216.
Ilg, A. K., Enkel, T., Bartsch, D., & Bähner, F. (2018). Behavioral effects of acute systemic low-dose clozapine in wild-type rats: implications for the use of DREADDs in behavioral neuroscience. *Frontiers in behavioral neuroscience*, 12, 173.
Jendryka, M., Palchaudhuri, M., Ursu, D., van der Veen, B., Liss, B., Kätzel, D., ... & Pekcec, A. (2019). Pharmacokinetic and pharmacodynamic actions of clozapine-N-oxide, clozapine, and compound 21 in DREADD-based chemogenetics in mice. *Scientific reports*, 9(1), 4522.
Johnson, P. L., Molosh, A., Fitz, S. D., Truitt, W. A., & Shekhar, A. (2012). Orexin, stress, and anxiety/panic states. *Progress in brain research*, 198, 133-161.
Josselyn, S. A., & Tonegawa, S. (2020). Memory engrams: Recalling the past and imagining the future. *Science*, 367(6473), eaaw4325.
Josselyn, S. A., Köhler, S., & Frankland, P. W. (2015). Finding the engram. *Nature Reviews Neuroscience*, 16(9), 521-534.
Kelley, M. J. (1985). Species-typical taxic behavior and event-reinforcer interactions in conditioning. *Learning and Motivation*, 16(3), 301-314.
Kessler, R. C. (2000). Posttraumatic stress disorder: the burden to the individual and to society. *Journal of Clinical Psychiatry*, 61, 4-14.
Kessler, R. C., Foster, C. L., Saunders, W. B., & Stang, P. E. (1995). Social consequences of psychiatric disorders, I: Educational attainment. *American journal of psychiatry*, 152(7), 1026-1032.
Kircher, T. T., Weis, S., Freymann, K., Erb, M., Jessen, F., Grodd, W., ... & Leube, D. T. (2007). Hippocampal activation in patients with mild cognitive impairment is necessary for successful memory encoding. *Journal of Neurology, Neurosurgery & Psychiatry*, 78(8), 812-818.
Kitamura, T., Ogawa, S. K., Roy, D. S., Okuyama, T., Morrissey, M. D., Smith, L. M., ... & Tonegawa, S. (2017). Engrams and circuits crucial for systems consolidation of a memory. *Science*, 356(6333), 73-78.
Klinzing, J. G., Niethard, N., & Born, J. (2019). Mechanisms of systems memory consolidation during sleep. *Nature neuroscience*, 22(10), 1598-1610.
Koch, M. (1999). The neurobiology of startle. *Progress in neurobiology*, 59(2), 107-128.
Konnopka, A., & König, H. (2020). Economic burden of anxiety disorders: a systematic review and meta-analysis. *Pharmacoeconomics*, 38(1), 25-37.

Konorski, J. (1949). Conditioned Reflexes and Neuron Organization. *Annals of Internal Medicine*, *31*(6), 1133. https://doi.org/10.7326/0003-4819-31-6-1133_1
Kubik, S., Miyashita, T., & Guzowski, J. F. (2007). Using immediate-early genes to map hippocampal subregional functions. *Learning & memory*, 14(11), 758-770.
Kumaran, D., Hassabis, D., & McClelland, J. L. (2016). What learning systems do intelligent agents need? Complementary learning systems theory updated. *Trends in cognitive sciences*, 20(7), 512-534.
Labiner, D. M., Butler, L. S., Cao, Z., Hosford, D. A., Shin, C. H. E. O. L. S. U., & McNamara, J. O. (1993). Induction of c-Fos mRNA by kindled seizures: complex relationship with neuronal burst firing. *Journal of Neuroscience*, 13(2), 744-751.
Lang, P. J., Bradley, M. M., & Cuthbert, B. N. (1997). Motivated attention: Affect, activation, and action. *Attention and orienting: Sensory and motivational processes*, 97, 135.
Lang, P. J., Davis, M., & Öhman, A. (2000). Fear and anxiety: animal models and human cognitive psychophysiology. *Journal of affective disorders*, 61(3), 137-159.
Lechner, H. A., Squire, L. R., & Byrne, J. H. (1999). 100 years of consolidation—remembering Müller and Pilzecker. *Learning & Memory*, 6(2), 77-87.
Linnman, C., Moulton, E. A., Barmettler, G., Becerra, L., & Borsook, D. (2012). Neuroimaging of the periaqueductal gray: state of the field. *Neuroimage*, 60(1), 505-522.
Liu, X., Ramirez, S., & Tonegawa, S. (2014). Inception of a false memory by optogenetic manipulation of a hippocampal memory engram. *Philosophical Transactions of the Royal Society B: Biological Sciences*, 369(1633), 20130142.
Liu, X., Ramirez, S., Pang, P. T., Puryear, C. B., Govindarajan, A., Deisseroth, K., & Tonegawa, S. (2012). Optogenetic stimulation of a hippocampal engram activates fear memory recall. *Nature*, 484(7394), 381-385.
Löw, A., Weymar, M., & Hamm, A. O. (2015). When threat is near, get out of here: Dynamics of defensive behavior during freezing and active avoidance. *Psychological science*, 26(11), 1706-1716.
MacLaren, D., Browne, R. W., Shaw, J., Radhakrishnan, S. K., Khare, P., España, R. A., & Clark, S. J. (2016). Clozapine N-Oxide Administration Produces Behavioral Effects in Long–Evans Rats: Implications for Designing DREADD Experiments. *ENeuro*, *3*(5), ENEURO.0219-16.2016. https://doi.org/10.1523/eneuro.0219-16.2016
Maeng, L. Y., & Milad, M. R. (2017). Post-traumatic stress disorder: The relationship between the fear response and chronic stress. *Chronic Stress*, 1, 2470547017713297.
Maren, S., Phan, K. L., & Liberzon, I. (2013). The contextual brain: implications for fear conditioning, extinction and psychopathology. *Nature reviews neuroscience*, 14(6), 417-428.
Martin, S. T., & Morris, R. V. (2002). New life in an old idea: The synaptic plasticity and memory hypothesis revisited. *Hippocampus*, 12(5), 609–636. https://doi.org/10.1002/hipo.10107
McNaughton, N., & Corr, P. J. (2004). A two-dimensional neuropsychology of defense: fear/anxiety and defensive distance. *Neuroscience & Biobehavioral Reviews*, 28(3), 285-305.
Morris, R. (1984). Developments of a water-maze procedure for studying spatial learning in the rat. *Journal of neuroscience methods*, 11(1), 47-60.
Müller, G., & Pilzecker, A. (1900). Experimentelle Beiträge zur Lehre vom Gedächtniss. In *Johann Ambrosius Barth eBooks*. http://ci.nii.ac.jp/ncid/BA58827975
Nagel, G., Ollig, D., Fuhrmann, M., Kateriya, S., Musti, A. M., Bamberg, E., & Hegemann, P. (2002). Channelrhodopsin-1: a light-gated proton channel in green algae. *Science*, 296(5577), 2395-2398.
Olatunji, B. O., Cisler, J. M., & Tolin, D. F. (2007). Quality of life in the anxiety disorders: a meta-analytic review. *Clinical psychology review*, 27(5), 572-581.
Park, H. J., & Friston, K. (2013). Structural and functional brain networks: from connections to cognition. *Science*, 342(6158), 1238411.
Patriquin, M. A., & Mathew, S. J. (2017). The neurobiological mechanisms of generalized anxiety disorder and chronic stress. *Chronic Stress*, 1, 2470547017703993.
Pentkowski, N. S., Blanchard, D. C., Lever, C., Litvin, Y., & Blanchard, R. J. (2006). Effects of lesions to the dorsal and ventral hippocampus on defensive behaviors in rats. *European journal of neuroscience*, 23(8), 2185-2196.
Phillips, M. L., Drevets, W. C., Rauch, S. L., & Lane, R. (2003). Neurobiology of emotion perception II: Implications for major psychiatric disorders. *Biological psychiatry*, 54(5), 515-528.
Pobbe, R. L. H., & Zangrossi Jr, H. (2010). The lateral habenula regulates defensive behaviors through changes in 5-HT-mediated neurotransmission in the dorsal periaqueductal gray matter. *Neuroscience letters*, 479(2), 87-91.
Pomrenze, M. B., Giovanetti, S. M., Maiya, R., Gordon, A. G., Kreeger, L. J., & Messing, R. O. (2019). Dissecting the roles of GABA and neuropeptides from rat central amygdala CRF neurons in anxiety and fear learning. *Cell reports*, 29(1), 13-21.

Ramirez, S., Liu, X., Lin, P. A., Suh, J., Pignatelli, M., Redondo, R. L., ... & Tonegawa, S. (2013). Creating a false memory in the HC. *Science*, 341(6144), 387-391.
Redondo, R. L., Kim, J., Arons, A. L., Ramirez, S., Liu, X., & Tonegawa, S. (2014). Bidirectional switch of the valence associated with a hippocampal contextual memory engram. *Nature*, 513(7518), 426-430.
Reijmers, L. G., Perkins, B. L., Matsuo, N., & Mayford, M. (2007). Localization of a stable neural correlate of associative memory. *Science*, 317(5842), 1230-1233.
Richmond, M. A., Yee, B. K., Pouzet, B., Veenman, L., Rawlins, J. N. P., Feldon, J., & Bannerman, D. M. (1999). Dissociating context and space within the hippocampus: Effects of complete, dorsal, and ventral excitotoxic hippocampal lesions on conditioned freezing and spatial learning. *Behavioral Neuroscience, 113*(6), 1189–1203. https://doi.org/10.1037/0735-7044.113.6.1189
Robbins, L., & Regier, D. A. (1991). *Psychiatric Disorders in America: How to Take Immediate Control of Your Mental, Emotional, Physical and Financial*. Simon and Schuste
Rosen, J. B., Pagani, J. H., Rolla, K. L., & Davis, C. (2008). Analysis of behavioral constraints and the neuroanatomy of fear to the predator odor trimethylthiazoline: a model for animal phobias. Neuroscience & *Biobehavioral Reviews*, 32(7), 1267-1276.
Ryan, T. J., Roy, D. S., Pignatelli, M., Arons, A., & Tonegawa, S. (2015). Engram cells retain memory under retrograde amnesia. *Science*, 348(6238), 1007-1013.
Saarni, S. I., Suvisaari, J., Sintonen, H., Pirkola, S., Koskinen, S., Aromaa, A., & Lönnqvist, J. (2007). Impact of psychiatric disorders on health-related quality of life: general population survey. *The British journal of psychiatry*, 190(4), 326-332.
Sauerhöfer, E., Pamplona, F. A., Bedenk, B., Moll, G. H., Dawirs, R. R., von Hörsten, S., ... & Golub, Y. (2012). Generalization of contextual fear depends on associative rather than non-associative memory components. *Behavioural brain research*, 233(2), 483-493.
Schacter, D. L., Eich, J. E., & Tulving, E. (1978). Richard Semon's theory of memory. *Journal of Verbal Learning and Verbal Behavior*, 17(6), 721-743.
Schmidt, M. V., Sterlemann, V., & Müller, M. B. (2008). Chronic stress and individual vulnerability. *Annals of the New York Academy of Sciences*, 1148(1), 174-183.
Schoderboeck, L., Wicky, H. E., Abraham, W. C., & Hughes, S. M. (2018). Genetic Targeting and Chemogenetic Inhibition of Newborn Neurons. *Human Gene Therapy Methods*, 29(6), 259-268. https://doi.org/10.1089/hgtb.2018.182
Scoville, W. B., & Milner, B. (1957). Loss of recent memory after bilateral hippocampal lesions. *Journal of neurology, neurosurgery, and psychiatry*, 20(1), 11.
Semon, R. (1925). The mneme. *The Journal of Nervous and Mental Disease*, *62*(3), 332.
Semon, R. W. (1904). *Die Mneme als erhaltendes Prinzip im Wechsel des organischen Geschehens, von Richard Semon*.
Senn, V., Wolff, S. B., Herry, C., Grenier, F., Ehrlich, I., Gründemann, J., ... & Lüthi, A. (2014). Long-range connectivity defines behavioral specificity of amygdala neurons. *Neuron*, 81(2), 428-437.
Sheng, M., & Greenberg, M. E. (1990). The regulation and function of c-fos and other immediate early genes in the nervous system. *Neuron*, 4(4), 477-485.
Shockett, P. E., & Schatz, D. G. (1996). Diverse strategies for tetracycline-regulated inducible gene expression. *Proceedings of the National Academy of Sciences*, 93(11), 5173-5176.
Soya, S., Shoji, H., Hasegawa, E., Hondo, M., Miyakawa, T., Yanagisawa, M., ... & Sakurai, T. (2013). Orexin receptor-1 in the locus coeruleus plays an important role in cue-dependent fear memory consolidation. *Journal of Neuroscience*, 33(36), 14549-14557.
Squire, L. R., Ojemann, J. G., Miezin, F. M., Petersen, S. E., Videen, T. O., & Raichle, M. E. (1992). Activation of the hippocampus in normal humans: a functional anatomical study of memory. *Proceedings of the National Academy of Sciences*, 89(5), 1837-1841.
Stein, M. B., & Kean, Y. M. (2000). Disability and quality of life in social phobia: epidemiologic findings. *American Journal of Psychiatry*, 157(10), 1606-1613.
Stosiek, C., Garaschuk, O., Holthoff, K., & Konnerth, A. (2003). In vivo two-photon calcium imaging of neuronal networks. *Proceedings of the National Academy of Sciences*, 100(12), 7319-7324.
Stuber, G. D., & Wise, R. A. (2016). Lateral hypothalamic circuits for feeding and reward. *Nature neuroscience*, 19(2), 198-205.
Sullivan, P. F., & Geschwind, D. H. (2019). Defining the genetic, genomic, cellular, and diagnostic architectures of psychiatric disorders. *Cell*, 177(1), 162-183.
Swanson, L. W., Sanchez-Watts, G., & Watts, A. G. (2005). Comparison of melanin-concentrating hormone and hypocretin/orexin mRNA expression patterns in a new parceling scheme of the lateral hypothalamic zone. *Neuroscience letters*, 387(2), 80-84.
Tejeda, H. A., & Bonci, A. (2019). Dynorphin/kappa-opioid receptor control of dopamine dynamics: Implications for negative affective states and psychiatric disorders. *Brain research*, 1713, 91-101.

Thompson, R. F. (2005). In search of memory traces. *Annu. Rev. Psychol*., 56, 1-23.
Tonegawa, S., Morrissey, M. D., & Kitamura, T. (2018). The role of engram cells in the systems consolidation of memory. *Nature Reviews Neuroscience*, 19(8), 485-498.
Tovote, P., Esposito, M. S., Botta, P., Chaudun, F., Fadok, J. P., Markovic, M., ... & Lüthi, A. (2016). Midbrain circuits for defensive behaviour. *Nature*, 534(7606), 206-212.
Tovote, P., Fadok, J. P., & Lüthi, A. (2015). Neuronal circuits for fear and anxiety. *Nature Reviews Neuroscience*, 16(6), 317-331.
Trivedi, M. A., & Coover, G. D. (2004). Lesions of the ventral hippocampus, but not the dorsal hippocampus, impair conditioned fear expression and inhibitory avoidance on the elevated T-maze. *Neurobiology of learning and memory*, 81(3), 172-184.
Tsvetkov, E., Carlezon, W. A., Benes, F. M., Kandel, E. R., & Bolshakov, V. Y. (2002). Fear conditioning occludes LTP-induced presynaptic enhancement of synaptic transmission in the cortical pathway to the lateral amygdala. *Neuron*, 34(2), 289-300.
Van Vreeswijk, C., & Sompolinsky, H. (1996). Chaos in neuronal networks with balanced excitatory and inhibitory activity. *Science*, 274(5293), 1724-1726.
VanElzakker, M., Fevurly, R. D., Breindel, T., & Spencer, R. L. (2008). Environmental novelty is associated with a selective increase in Fos expression in the output elements of the hippocampal formation and the perirhinal cortex. *Learning & memory*, 15(12), 899-908.
Vernet-Maury, E., Polak, E. H., & Demael, A. (1984). Structure-activity relationship of stress-inducing odorants in the rat. *Journal of Chemical Ecology*, 10(7), 1007-1018.
Vetere, G., Tran, L. M., Moberg, S., Steadman, P. E., Restivo, L., Morrison, F. G., ... & Frankland, P. W. (2019). Memory formation in the absence of experience. *Nature neuroscience*, 22(6), 933-940.
Vos, T., Abajobir, A. A., Abate, K. H., Abbafati, C., Abbas, K. M., Abd-Allah, F., ... & Criqui, M. H. (2017). Global, regional, and national incidence, prevalence, and years lived with disability for 328 diseases and injuries for 195 countries, 1990–2016: a systematic analysis for the Global Burden of Disease Study 2016. *The Lancet*, 390(10100), 1211-1259.
Watson, D., & Clark, L. A. (1984). Negative affectivity: the disposition to experience aversive emotional states. *Psychological bulletin*, 96(3), 465.
Weissman, M. M. (1991). Panic disorder: impact on quality of life. The Journal of clinical psychiatry.
Whitaker, L. R., & Hope, B. T. (2018). Chasing the addicted engram: identifying functional alterations in Fos-expressing neuronal ensembles that mediate drug-related learned behavior. *Learning & Memory*, 25(9), 455-460.
Yu, J. Y., Fang, P., Wang, C., Wang, X. X., Li, K., Gong, Q., ... & Wang, X. D. (2018). Dorsal CA1 interneurons contribute to acute stress-induced spatial memory deficits. Neuropharmacology, 135, 474-486.
Zhong, J., Liang, M., Akther, S., Higashida, C., Tsuji, T., & Higashida, H. (2014). c-Fos expression in the paternal mouse brain induced by communicative interaction with maternal mates. *Molecular brain*, 7(1), 1-11.
Zhou, Y., Won, J., Karlsson, M. G., Zhou, M., Rogerson, T., Balaji, J., ... & Silva, A. J. (2009). CREB regulates excitability and the allocation of memory to subsets of neurons in the amygdala. *Nature neuroscience*, 12(11), 1438-1443.

6. Appendix

6.1 Implant surgery protocol

- **Prep Stereotax/Needle (two needles needed for this surgery)**
  - Fill Hamiltons w/ mineral oil (copper needle); slowly without bubbles
    - Always check the needle is clean and clear; use ethanol to pull up in the needle 4 times before using. Feel free to soak the needle itself and cap in the ethanol for a few minutes. Once the stream of EtOH is clean and clear, fill with mineral oil below.
    - To fill with mineral oil, remove the needle tip and screw holding the needle tip from the Hamilton. Pull the plunger to about 400 nL, and insert the mineral oil floppy needle into the opening of the Hamilton you've just made
    - Keep constant pressure as you pull the mineral oil syringe out of the Hamilton to keep the whole thing filled with mineral oil (no bubbles!)
    - Load the Hamilton into the stereotax, making sure to tighten the knob at the top to apply even pressure to your plunger
  - Parafilm w/ virus (repeat for each needle with different viruses)
    - Before pulling up the virus, always expel 100nL of mineral oil at 50nL/sec to get rid of any tiny air bubbles you can't see.
    - Lower needle down into bubble of virus
    - Withdraw (500nL; 50SLN; repeat until all is removed; 3-5 times)
      - *write down the total virus volume you have to work with*
  - Inject 25-50nL until you see a small bubble at the tip; test it's coming out
  - Move needle out of the way
- **Fill out surgery sheet**
  - Cage #, body weight, infusion only, name, surgery start time
- **Get started!**
  - Turn on heating pad (LOW); paper towels under mouse to prevent overheating
- **Induce mouse**
  - Open black valve near wall
  - Open OXYGEN valve (left)
  - Start flow rate (1.2); turn knob
  - Check flow is going to induction chamber
  - Turn on iso to 3% ish for induction
  - Put mouse in induction chamber; wait until not moving; breathing slows
- **Move mouse to stereotax quickly**
  - Switch over valve to nose cone; lower iso to 2%
  - Scruff; use Q-tip to roll out tongue
  - Adjust teeth, making sure they're in the notch; lock nose cone over snout
  - Adjust ear bars until head is stable; you'll feel the bar enter a little notch in the skull.
- **Prep for opening**
  - **Lidocaine (0.1mL)** under scalp
  - Veet/Nair on head with Q-tip (sit 30 sec); wipe with gauze/Q-tips to remove hair
  - Wash 3x (betadine/alcohol); in-out with Q-tips
  - Paralube on eyes (Q-tip)
- **Open head**
  - Use tweezers to hold scalp skin; cut teardrop shape with scissors to remove a little flap of skin.
  - Pull tissue apart/widen the hole with two Q-tips
  - Gently remove the excess tissue on the sides of the incision so the headcap is flush against the skin.
  - Scrape skull with tweezers to remove excess tissue/allow for metabond to hold later.
- **Give meloxicam (0.2-0.3mL, depending on weight);** tent skin on back
- **Level brain**
  - Pivot needle over head; lock in place at 0

- Bregma (top); zero out coordinates.
- Lambda (bottom); within 0.05mm (try as close to 0 mm as possible)
- Redo if needed; move head up/down to accommodate.
- Check left and right for leveling as well - choose a random point on left/right hemispheres and make sure DV is the same (within 0.15mm).

- **Drill all holes** - use drill attachment and stereoscope.
- **Inject all holes** -
  - Virus 1 for fiber photometry
    - Put the needle into the stereotax
    - Re-bregma the needle
    - Go to the injection site (should be over the hole you drilled)
    - Lower needle to 0.05 below the injection site (slightly lower for a second to create a pocket for the virus) wait 3 mins; then back up to -4.5DV and wait 1 min. (inject here)
    - Wait 6-7 minutes with the needle in place
    - Slowly remove needle
      - Check virus is coming out (50nL; 50SLN)
  - Virus 2 for optogenetics
    - Put the other needle into the stereotax
    - Re-bregma the needle
    - Go to the left injection site
    - Lower needle to 0.05 below the injection site (slightly lower for a second to create a pocket for the virus) wait 3 mins; then back up to -4.5DV and wait 1 min. (inject here)
    - Wait 6-7 minutes with the needle in place
    - Slowly remove needle
      - Check virus is coming out (50nL; 50SLN)
    - Repeat on the right side of the skull.
- **Implant holes:**
  - Fiber photometry implant 1
    - Change attachment (fiber implant holder); place fiber in the twisty part but don't secure it too tight--will be hard to remove!
    - Re-bregma (tip of fiber should be placed at bregma, zero coordinates, go back to lambda and it should be pretty close ML/AP)
    - Go over to the coordinates of the implant and it should line up!
    - **Lower implant** very slowly to the DV coordinates
    - **DRY SKULL w/ Q-tip**
    - **Metabond** this fiber in place
      - Powder, liquid, catalyst (one drop); work quickly!
      - Be sure to not get this metabond all over the skull/in the other implant hole.
      - Wait 5-7 mins to dry
    - **Dental cement** a little 'ant hill' around the implant to secure it further
      - Mix powder and liquid until desired consistency
      - Work quickly; you can wait a tiny bit if you need it to be thicker/less liquidy.
      - Wait 5-7 mins to dry
    - When everything has dried/you have the confidence to **remove the holder**--go for it!
      - Twist the holder clockwise to gently release the implant
      - Watch to make sure the fiber itself isn't moving/you don't pull it out of the skull.
  - Optogenetics implants
    - Change attachment (dual fiber holder); place fiber in the twisty part but don't secure it too tight--will be hard to remove!

        - Re-bregma (tip of fiber should be placed at bregma, zero coordinates, go back to lambda and it should be pretty close ML/AP)
        - Go over to the coordinates of the implant and it should line up!
        - **Lower implants** very slowly to the DV coordinates
        - **Metabond** these fibers in place
            - Powder, liquid, catalyst (one drop); work quickly!
            - Be sure to not get this metabond all over the skull/in the other implant hole.
            - Wait 5-7 mins to dry
        - **Dental cement** a little 'ant hill' around the implant to secure it further
            - Mix powder and liquid until desired consistency
            - Work quickly; you can wait a tiny bit if you need it to be thicker/less liquidy.
            - Wait 5-7 mins to dry
        - When everything has dried/you have the confidence to **remove the holder**--go for it!
            - Twist the holder clockwise to gently release the implant
            - Watch to make sure the fiber itself isn't moving/you don't pull it out of the skull.
    - **Build your headcap up a little bit more**
        - Metabond w/ one drop catalyst on the entire surface of the skull/screw
            - Allow to dry 5-7 mins
        - Dental cement and build up a little cap around the fibers
            - Leave enough room exposed on the fibers to plug in patch cord later.
            - Allow to dry for 5-7 mins.
        - Once dry, write animal ID# on the headcap with a permanent marker.
- **Set up recovery cages**
    - Heating pad LOW-MED; place cage half on.
    - Prop cages up with paper towels so it's level.
    - Paper towel inside
    - Gel + food on floor
- **Admin saline (0.2-0.3mL)** and **buprenorphine (0.1mL)** on back subQ; tent skin
- **Post-surgery**
    - Turn off iso; give oxygen for 1-2 mins ("0" on the iso machine if needed)
    - Put in the recovery cage; monitor until moving.
    - Fill out the surgery sheet (end time; check boxes; final weight; any important notes); surgery card on the new cage.
    - Place mouse back in new clean cage once awake
- **Q: Do I need more virus? Do I need to refill iso?**
    - If yes, clean hamilton w/ EtOH and refill with virus
    - If yes, turn off oxygen completely to fill iso; DO NOT FILL WHEN O2 IS RUNNING.

6.2 Fiber photometry protocol

1. What type of experiment are you running today?
    1. FreezeFrame
        1. Turn on the computer (right side of the room)
        2. Log-in to your account
        3. Select FreezeFrame4 application on the Desktop
        4. Select Recorder
        5. You will see two cameras (left should be video, right is black)
            1. The left box on the screen is currently the right-most box that we use for FC.
            2. Save a new file path so you don't overwrite someone's data
        6. Now (if you're fear conditioning), you will **turn on the shock box** (again, make sure you're turning on the box to the right). The power button is on the back. When it is on, there will be a little red light.
            1. Test your shocker/set the intensity in mA.
            2. We normally want 1.5mA intensity with the switch on HIGH
            3. To check this, you will move the switches to "Set/Test" and "Manual"
            4. When you manually move and hold the switch, the little needle on the mA will go to 1.5mA ideally.
            5. If this is not the case, you will adjust the little knob up or down until the desired intensity is reached.
            6. **Note:** there is also a LOW setting on the shocker, this is NOT what we want and this uses the top row of mA values.
        7. Clean the chamber and bottom tray with 70% EtOH before and in between testing! This is super important. They will smell each other's fear (sad).
        8. To start a session when you're ready to record:
            1. Before you put a mouse in the FC box for recording, you will need to name the individual file that corresponds to the correct box 2; name it something specific like **'FP_pilot_shock_mouse1_FC'**
            2. Select the correct protocol from the drop-down menu; we normally use **"5:30 4-shock"** for fear conditioning, **"5:30 no shock"** for recall, and "**30 min extinction"** for extinction sessions.
            3. To start the session later, you will place the mouse in the box, close and lock the front door, press "Reference" and "Start".
            4. We usually start the NPM recording, count one-two-three and then start the session on FreezeFrame.
        9. Now you're ready to set up the NPM box!
2. Setting up the NPM Box
    1. Plug in the power cord from the NPM box to the wall
    2. Turn on the computer (left side of the room); it should usually be off.
    3. Turn on the power switch on the left side of the box, you will hear it begin to make noise and the screen will turn on.
    4. Take the cord that is wrapped up on the shelf and plug the USB into the bottom right port on the FP computer (COM5) - this is for room b only
        1. Room c - top left port is COM5
        2. Other computers - you'll have to figure it out
    5. Log-in to computer account (ask Rebecca or Kaitlyn or Ryan for password)
    6. Open Bonsai - *don't ask me why* but just go into the search box and search "Bonsai" instead of selecting the application itself on the desktop.
    7. Once it opens, select "Open Project" *again, don't ask me why* but do NOT select from the recent list.

8. Go into Desktop < Bonsai Workflows < Ryan_Workflow_Experimental_REBECCA

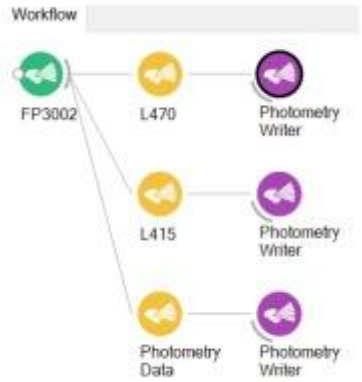

(room b)
    1. Room C - REBECCA in all caps is the correct protocol
9. The green “PLAY” button should appear on the NPM box on the little screen (area i from the above diagram)

3. Set-up your FP3002 Node
    1. Double click on the node itself “FP3002”
    2. A window should open! You should not get any errors here, but if you do, follow these steps in any random order:
        1. *try closing Bonsai and re-opening it
        2. *try unplugging the USB and plugging it back in, then re-open Bonsai

        3. *try turning off the NPM box and start over
        4. *if it’s really bad, you’ll have to turn everything off/unplug and begin again.
        5. Once you’ve sacrificed your soul to the neurophotometrics gods, continue.
    3. Set the **Trigger Sequence** (in this exact order):
        1. 470, 415, None - for single color GCaMP recordings
        2. 470, 560, 415 - for dual color GCaMP and jRGECO recordings
           ** If you accidentally created more channels than wanted and want to delete a channel, have to select the one <u>above</u> and press Delete button
    d. Change the **Frame Rate**

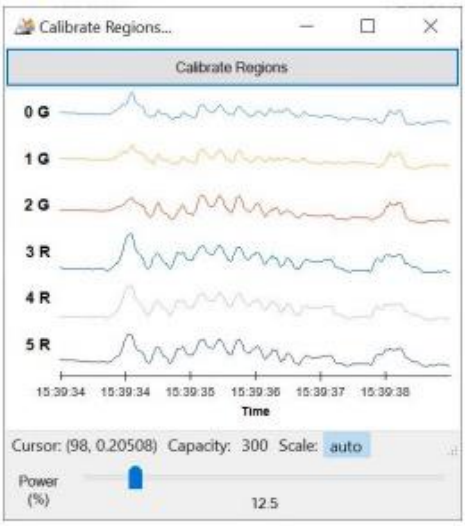

1. Usually 28 FPS or 56 FPS depending on your moral belief system

d. Calibrate Regions

2. Select the button on the left side of the window
3. Another window will open, showing a blue trace that's just vibing~
4. You will select the "Calibrate Regions" button at the top of this window.
5. If there are leftover circles from last time, select them with your mouse and press delete button.
6. Two illuminated circles (these are the ends/tips of your patch cords) will appear on the left and right sides of the window.
    1. *Note: the circles should be bright, crisp and have no fuzzy edges
    2. This is where you go back and re-check the connection to the laser/magnet itself. If it is misaligned, this can cause this issue. WEAR LASER GOGGLES when near the laser always.
7. You can tap the end of the patch cord with a gloved finger or shine light down the tip to better illuminate the ROI. Select the button on the left side of the window
8. Another window will open, showing a blue trace that's just vibing~
9. You will select the **"Calibrate Regions"** button at the top of this window.
10. Two illuminated circles (these are the ends/tips of your patch cords) will appear on the left and right sides of the window.

11. *Note: the circles should be bright, crisp and have no fuzzy edges
    1. This is where you go back to Step 2 above and re-check the connection to the laser/magnet itself. If it is misaligned, this can cause this issue. **WEAR LASER GOGGLES** when near the laser always.
    2. You can tap the end of the patch cord with a gloved finger or shine light down the tip to better illuminate the ROI.
12. Left click and drag over each circle to generate red and green ROIs.
    1. You want these to be as perfectly aligned over the original circles as possible.
    2. As you add these circles, you will see traces appear *(orange and blue usually)* on the original window. Ideally, these traces will be clean, flat and close to the center, running parallel to one another.
    3. You can right click and drag to re-define the ROI size or location.

4. To delete an ROI, left click on the ROI and hit delete on your keyboard.
5. You can increase the power slider on the bottom of the window to ~ 8-11% to see what your traces will look like.
6. In the example above, they use a branching patch cord (two), which is why there are two ROIs per side--we also use this kind, but keep the other branch in the dark NPM fiber box on the shelf so you won't see the second set of ROIs.

13. You can close the Regions and Calibrate Regions windows when done!

d. Calibrate Power

14. In the original FP3002 window, this "Calibrate Power" button will be located on the left.
15. Obtain laser goggles, sensor and power meter from the cabinets outside in the behavior hallway.
16. Turn off all the lights in the room, you can leave the red ones on if you need it!
    1. Unscrew the lid on the sensor and plug it into the power meter.
    2. Turn the power meter on and select the correct wavelength (415, 470, 520)
17. In this window, you will see 3 slider bars; each defines the amount of amperage sent to each individual LED as a percentage %.
18. To calibrate power, slide one slider to a % and use a power meter to configure; out of the fiber tip, the power should be ~50uW or 0.05mW for all LEDs and 200um patch cords.
19. Bring the slider back to zero when testing a different LED.
20. Write these numbers down on the whiteboard (470, 560 or 415 only)
21. When you close out the Calibrate Power window, the numbers you wrote down should be entered into the Power Configuration Table.
22. Enter 0 for the 560 nm LED if you are not using it!

d. Save Device Settings…

23. On the left hand side of the FP3002 Setup window, select the "Save Device Settings…" button.
24. You can overwrite an old FP3002Config_RS
25. *DO NOT save the register values on persistent device memory*
26. Close out of the FP3002 Setup window.

d. AutoCrop

27. On the right hand side of the Bonsai window, there will be Properties and Misc. Under Misc, there is AutoCrop.
28. AutoCrop should be set to True if the frame rate is above 80 frames/sec.
29. If not, it should be set to False. We normally collect at lower frame rates than this, so we set it to FALSE.
30. You can set this by double clicking on True/False in the right panel of the workflow window.

d. Plug in the Webcam

31. Adjust so the testing box is in frame
32. Plug in the USB for the webcam to the bottom left (only open USB remaining)
33. Set Camera FrameRate
34. Click on the VideoWriter node
35. On the right hand Bonsai window, you will see FrameRate = 30 probably. Click on it and type 28 or your desired FPS (this must match the frame rate of collection that you previously set in the FP3002 node.
    1. Please note: your webcam may 'tap out' at a lower FPS than you type here; it will default
36. You're now ready to collect FP data!

4. **Begin Testing**
    1. Plug in your mouse gently and place into the respective chamber
    2. Start the Bonsai recording session by pressing START in the top left of the interface.
    3. Begin the FreezeFrame at the same time as pressing the spacebar on theBonsai computer to record the timestamp for the beginning of the session.
    4. Double click on the 415 and 470 nodes, as well as the Camera nodes to see the live data.
5. **After Testing Ends…**
    1. Press the STOP button twice in Bonsai to end the recording.
    2. Save your files!
        1. They will be automatically saved in the Test folder on the Desktop
        2. Rename these files to whatever you want (i.e. BLA_C2_FC_M6)
        3. IF YOU FORGET, YOU WILL OVERWRITE YOUR DATA WITH THE NEXT MOUSE!!
    3. Move your files to Google Drive < Fiber Photometry folder
6. **Cleaning up!**
    1. Turn off the NPM system (power button), unplug the power source from the wall outlet and unplug the USB cable at the end of each day.
    2. This will avoid overheating the camera.

6.3 Confocal microscope protocol

Confocaling 101: Zeiss Microscope

1. **Power on confocal**
    1. Turn on power strip
    2. Turn laser Key from O to I
    3. Turn on System and Components switches on box above laser key
    4. If using camera, turn on camera
    5. Turn on Computer
    6. Open Zen Blue, select Zen System
    7. Allow hardware to connect and 'Calibrate Now' when prompted
2. **Microscope (eyepiece)**
    1. Make sure you are on **Locate Tab** within the Zen software
    2. Select (10x, 20x, 40x oil, 60x oil) objective on the touch screen
        1. *I.e. if using oil objective* = place rubber band around lens and drop oil onto top; clean with lens cleaner/special wipe paper on left side of confocal.
3. **Put slide in microscope**
    1. Face down--top of the slide should remain facing the top (towards the wall behind the confocal).
4. **Microscope (eyepiece)**
    1. Locate area of interest using joystick and fine adjustment
    2. Check all channels for expression (usually on 10x)
        1. You have to individually click each channel button under Locate Tab (DAPI, GFP, Cy3, Cy5, All Off) in the software.
5. **Acquisition tab** within the Zen software
    1. *wait for beep* before clicking **LIVE**
    2. Check off z-stack or tiles if you want them!
    3. LIVE image
        1. Check yo cells
    4. **Acquisition Mode**
        1. 1024px X 1024px (frame size)
        2. 8 bits/pixel is standard
        3. 8-9 = scan speed; faster scan speed = faster imaging = lower quality image
        4. Avg = 2 (increase avg, slower, better image)
        5. Scan area = 1.0x typically
            1. If you're doing whole brain slice = 0.6x (larger pixel size)
            2. If you want high quality = 1.0x
    5. **Tiles -**
        1. Delete old tiles (trash can button)
        2. Set your desired tile size (e.g. 3x5)--then press the Advanced setup button--then press the + button to drop your tile into the region.
        3. *for full sagittal slices → recommended tips*
            1. Once in Advanced Set-up, drop random tile size into the space
            2. Go back to Locate Tab<DAPI channel
            3. Use the joystick and microscope to navigate to the edges of the huge slice
            4. Adjust the tile size with the mouse as needed
            5. This gives you a pretty good outline of the slices without wasting too much time.
            6. Now, go back to Acquisition Tab < LIVE
    6. **Channels**
        1. DAPI (blue), dsRed (red), EGFP (green), Cy5 (far red)
        2. Check or uncheck the boxes to use them
        3. Clicking on each of these will allow you to adjust its parameters (laser nm, pinhole, master gain, digital offset, digital gain).
            1. Generally speaking...laser nm makes things brighter, pinhole gives you a sharper image, master gain increases saturation, digital offset decrease will get rid of the fuzziness, and digital gain increase will increase all those parameters...just mess around with them!
            2. When imaging the same slide, you want to keep the actual laser settings the same (laser power, pinhole), but you can modify the digital settings (gain, etc.)

7. **Snap**
    1. Takes a single image plane of all channels where you are currently located
    2. Usually do this before committing to an image
8. **Z-stack!**
    1. Set first and last (*note: first is bottom, last is top); use the fine focus to do this
        1. "UP" in the stack is scrolling towards the wall
        2. "DOWN" in the stack is scrolling away from the wall; towards you.
    2. Check for all channels to make sure all color is included in your stack
    3. You can adjust slice number by changing the interval (um); usually we take 5-12
    4. Slices depending on what you want → less slices = faster imaging
9. **Focus Strategy -**
    1. First pull-down menu = "None" instead of "Software Autofocus"
    2. Fixed Z should be selected
10. **Start experiment** (see time, set timer)

6. Saving Images
    1. Right click on the tab "Experiment whatever" and save as .czi file
7. Cleaning up
    1. Close Zen Software
    2. Shut down computer
    3. Laser key to O
    4. Turn off system/components switches
    5. Turn off power strip